

This work was written as part of one of the author's official duties as an Employee of the United States Government and is therefore a work of the United States Government. In accordance with 17 U.S.C. 105, no copyright protection is available for such works under U.S. Law.

Public Domain Mark 1.0

<https://creativecommons.org/publicdomain/mark/1.0/>

Access to this work was provided by the University of Maryland, Baltimore County (UMBC) ScholarWorks@UMBC digital repository on the Maryland Shared Open Access (MD-SOAR) platform.

Please provide feedback

Please support the ScholarWorks@UMBC repository by emailing scholarworks-group@umbc.edu and telling us what having access to this work means to you and why it's important to you. Thank you.

Measurement of the Rugged Invariants of Magnetohydrodynamic Turbulence in the Solar Wind

WILLIAM H. MATTHAEUS AND MELVYN L. GOLDSTEIN

*Interplanetary Physics Branch, Laboratory for Extraterrestrial Physics, Goddard Space Flight Center
Greenbelt, Maryland 20771*

Measurements of the total energy, cross helicity, and magnetic helicity of the solar wind at 1, 2.8, and 5 AU are presented. These quantities are the three rugged invariants of three-dimensional ideal incompressible MHD turbulence theory. The theoretical technique for measuring the magnetic helicity from the matrix of two-point correlations is shown. The length scales characterizing the magnetic helicity are found to be equal to or greater than those which characterize the magnetic energy. The magnetic helicity typically lies at scales larger than the magnetic correlation length, consistent with the expectations of the inverse cascade and selective decay hypotheses of three-dimensional MHD turbulence. At smaller scales, the magnetic helicity oscillates in sign. Our measurements of the cross helicity are not fully consistent with the usual interpretation in terms of outward propagating Alfvénic fluctuations. Especially during the interval at 5 AU the cross helicity is found to oscillate in sign indicating fluctuations propagating both outward and inward.

1. INTRODUCTION

In recent years, more experimental data have been accumulated in the solar wind than perhaps in any other magnetized plasma of either natural or man-made origin. The availability of these data has made possible a great increase in theoretical understanding of the solar wind. Many of the recent advances and outstanding problems in solar wind research have been reviewed by *Hundhausen* [1972] and *Holzer* [1979]. In studies of the macroscopic properties of the interplanetary plasma one has more often than not been able to neglect the role of the fluctuating magnetic and velocity fields on the large-scale structure of the solar wind, arguing that the dominant energy source is the super-Alfvénic kinetic energy of the flow. However, as is well known from studies of hydrodynamic turbulence and as has been conjectured for magnetohydrodynamic (MHD) turbulence, nonlinear interactions of small-scale fluctuations can produce signatures at large scales.

In this paper we begin an investigation of the statistical properties of solar wind fluctuations with the goal of understanding the fluctuation spectra of the magnetic and velocity fields and their relationship to macroscopic structure. The basic theoretical model which we use to organize this investigation is to consider the solar wind as a turbulent MHD fluid. Another objective is to investigate the extent to which this model is appropriate. To that end we have analyzed solar wind plasma and field data in terms of several characteristic parameters of the simplest possible turbulence model, namely, incompressible, single-fluid MHD. This choice is a compromise; the solar wind is known to exhibit fluctuations in density and to have comparable sound and Alfvén speeds, whereas in a truly incompressible fluid the sound speed would greatly exceed the Alfvén speed. Moreover, the solar wind plasma certainly exhibits kinetic effects and many of the phenomena in the wind can only be understood in terms of a multifluid model. However, the incompressible single-fluid model is probably the best devel-

oped fluid turbulence model owing much to analogy with the success in hydrodynamic turbulence of relating observations of turbulent fluids [*Grant et al.*, 1962] to theoretical expectations (see, for example, *Batchelor* [1970]). In addition, a two-dimensional MHD model has been studied using numerical simulations [e.g., *Fyfe et al.*, 1977; *Kraichnan and Montgomery*, 1980]. Despite obvious limitations, the single-fluid incompressible model has been widely used in dynamo theory [*Moffatt*, 1978] and various astrophysical applications [*Parker*, 1979].

Many previous observational and theoretical studies of solar wind fluctuations have adopted the complementary point of view that the fluctuations can be described as a superposition of MHD waves and stationary structures. This work has been reviewed by *Barnes* [1979], who points out that the wave and turbulence approaches are not entirely incompatible. Indeed, the approaches perhaps differ largely in style and vocabulary, but with regard to some issues they may yield entirely different perspectives.

One of the important questions one would eventually like to answer is to what extent nonlinear interactions are presently active, and to what extent the observed fluctuations are inert remnants of processes occurring very near the sun. *Coleman* [1968] argued that inhomogeneity of the mean plasma outflow provides an unstable shear flow to drive turbulence. Ongoing turbulence, including fluctuations ranging from the scale size of the system (≈ 1 AU) to the dissipative small scales (the ion gyroradius, or smaller), implies a direct transfer of energy from large to small scales and, perhaps, an inverse cascade of some fraction of the energy from small scales to large.

There are theoretical arguments suggesting that the nonlinear turbulence processes significantly affect the state of the largest-scale structures in a turbulent fluid. In the dual cascade [*Frisch et al.*, 1975] and selective decay hypotheses [*Matthaeus and Montgomery*, 1980], three-dimensional MHD turbulence is thought to proceed in such a way as to rapidly dissipate energy, but only at the expense of the appearance of nondecaying large-scale helical magnetic structures. It is entirely possible that the large-scale structure of a nonlinearly active solar wind can be understood only by including such features of turbulence.

Copyright 1982 by the American Geophysical Union.

Paper number 2A0804.
0148-0227/82/002A-0804\$05.00

The turbulence literature reveals that the basic theoretical vocabulary emphasizes the role of the quadratic ('rugged') integral invariants of the nondissipative, ideal MHD model: total energy, magnetic helicity, and cross helicity. Because the value of rugged invariants cannot be directly modified by nonlinear effects, their wave number spectra give valuable information about the state and dynamics of the turbulent magnetofluid.

In the sections that follow, we begin a description of solar wind fluctuations in terms of these rugged invariants. In section 2 the MHD model is described and the three invariants are defined and discussed. We demonstrate that the invariants are preserved by the ideal equations and discuss the role of boundary conditions and the notion of ruggedness. In section 3 we define the spectra of the invariants in the context of homogeneous turbulence. We show in detail that the magnetic helicity is measurable and present the basic formulas connecting it with experimental measurements. In section 4 the basis of the data analysis technique is described. The 'frozen-in-flux' approximation is examined, along with the conditions necessary for compatibility with the homogeneity assumption. Section 5 contains the results of our analysis of several intervals of Voyager magnetometer and plasma data. Energy, magnetic helicity and cross-helicity spectra are presented and discussed. The results are summarized in section 6.

2. INTEGRAL INVARIANTS IN MAGNETOHYDRODYNAMIC TURBULENCE

If a conducting fluid is incompressible and both the resistivity and the viscosity are spatially uniform and time independent, the MHD equations [Cowling, 1976] can be written in the form

$$\frac{\partial \mathbf{b}}{\partial t} = \nabla \times (\mathbf{v} \times \mathbf{b}) + \mu \nabla^2 \mathbf{b} \quad (1)$$

$$\frac{\partial \mathbf{v}}{\partial t} + (\mathbf{v} \cdot \nabla) \mathbf{v} = -\nabla P + \mathbf{J} \times \mathbf{b} + \nu \nabla^2 \mathbf{v} \quad (2)$$

$$\nabla \cdot \mathbf{v} = 0 \quad (3)$$

$$\nabla \cdot \mathbf{b} = 0 \quad (4)$$

where $\mathbf{J} = \nabla \times \mathbf{b}$ is the electric current density, and the notation has been simplified by defining the magnetic field \mathbf{b} in Alfvén speed units, where $\mathbf{b} \equiv \mathbf{B}/(4\pi\rho_0)^{1/2}$ (ρ_0 is the mean density).

Note that in (2), both the pressure and the electric current have been redefined using the fact that the density is constant. For example, $\mathbf{J} = (4\pi/\rho_0)^{1/2} \mathbf{j}$ where $\mathbf{j} = (c/4\pi) \nabla \times \mathbf{B}$. Both the resistivity μ and the viscosity ν have dimensions of (length)²/time, as is typical of transport coefficients. When written in this way, the MHD equations can be related in a straightforward way to a system of dimensionless units in which μ and ν play the role of inverse magnetic Reynolds numbers and inverse mechanical Reynolds numbers, respectively. This system of units is often used in computer simulations of MHD turbulence [e.g., Matthaeus and Montgomery, 1981; Fyfe and Montgomery, 1976] and is described further in Appendix A. Equation (3) can be regarded as a dynamical constraint corresponding to incompressibility and uniform density, while (4) may be viewed as an initial condition on the magnetic field.

When an MHD fluid is turbulent, the detailed behavior of the solutions $\mathbf{b}(\mathbf{x}, t)$ and $\mathbf{v}(\mathbf{x}, t)$ becomes analytically inaccessible even if boundary and initial data are precisely known. In these circumstances the only description available is a statistical one. One invaluable tool in constructing a statistical description is knowledge of the invariants of the 'ideal' model equations of motion (i.e., those for which $\mu = \nu = 0$). The invariants most useful in describing turbulence are the integral invariants quadratic in \mathbf{v} and/or \mathbf{b} . There are only three known quadratic invariants of the ideal system [Frisch *et al.*, 1975]. These are the energy (per unit density)

$$E = (1/2) \int d^3x (\mathbf{v}^2 + \mathbf{b}^2) \quad (5)$$

the cross helicity

$$H_c = (1/2) \int d^3x \mathbf{v} \cdot \mathbf{b} \quad (6)$$

and the magnetic helicity

$$H_m = \int d^3x \mathbf{A} \cdot \mathbf{B} \quad (7)$$

\mathbf{A} is the magnetic vector potential which defines \mathbf{B} via the relation $\mathbf{B} = \nabla \times \mathbf{A}$. Note that in (5) and (6) the magnetic field in Alfvén units, \mathbf{b} , is used (see Appendix A). We shall use this convention when discussing total energy or cross helicity, but comparisons of magnetic helicity (7) with magnetic energy are more conveniently done using \mathbf{B} in ordinary cgs units (see (9), (13), and (19)). For convenience, and unless otherwise stated, we will usually work in the Coulomb gauge, $\nabla \cdot \mathbf{A} = 0$. Normally, the domain of integration in (5)–(7) extends over the entire plasma-containing region D . We denote by S the surface which bounds D .

Any proof of the invariance of E , H_c , and H_m for the ideal MHD equations depends rather critically on the nature of the boundary conditions chosen for \mathbf{v} and \mathbf{b} on the surface S . The general procedure is to reduce time derivatives of the invariants to surface terms. Invariance then follows for those boundary conditions for which the surface terms vanish. The invariants of the compressible MHD equations were first discussed by Woltjer [1958a, b]. Because the invariants play such a central role in the remainder of this paper and because Woltjer's papers do not seem to be well known, we briefly review the proofs for ideal incompressible MHD.

First consider the invariance of E . From (1) and (2) we have (recall $\mu = \nu = 0$)

$$\frac{dE}{dt} = -\int dS \hat{\mathbf{n}} \cdot \mathbf{v} (v^2/2 + P) + \int dS \hat{\mathbf{n}} \cdot [(\mathbf{v} \times \mathbf{b}) \times \mathbf{b}]$$

where $\hat{\mathbf{n}}$ is an outward directed unit normal to the boundary surface and dS is the local differential area element. Note that because $\mathbf{E} = -\mathbf{v} \times \mathbf{B}$ in ideal MHD, the second integral is the Poynting flux across the surface, while the first integral represents the flux of kinetic energy and pressure across the boundary. It is apparent that E is a constant in time if any one of several boundary conditions is imposed. These include $\hat{\mathbf{n}} \cdot \mathbf{b} = 0$ and $\hat{\mathbf{n}} \cdot \mathbf{v} = 0$, corresponding to a perfectly conducting and free slip boundary on S . A second class of suitable boundary conditions is $\mathbf{v} = 0$ on S . The third class is periodic boundary conditions in a large box. In this case, \mathbf{v} , \mathbf{B} , and P are assumed periodic so that the surface terms, while not identically zero, vanish due to cancellations. This establishes the invariance of total energy.

The conditions for invariance of the cross helicity may be determined in a similar manner. Equations (1) and (2) can be

combined to give

$$2 \frac{dH_c}{dt} = - \int dS (\hat{n} \cdot \mathbf{v}) (\mathbf{v} \cdot \mathbf{b}) + \int dS (\hat{n} \cdot \mathbf{b}) (v^2/2 - P)$$

Again, invariance is established when $\mathbf{v} \cdot \hat{n} = 0$ and $\mathbf{B} \cdot \hat{n} = 0$ on S ; or, alternatively, when $\mathbf{v} \cdot \mathbf{b}$ and $(v^2/2 + P)$ are periodic. H_c is also invariant if $\mathbf{b} = 0$ on S .

The invariance of the magnetic helicity is most easily examined by considering the equation for \mathbf{A} obtained by 'uncurling' (1)

$$\frac{\partial \mathbf{A}}{\partial t} = \mathbf{v} \times \mathbf{B} - \nabla \Psi \quad (8)$$

Note that in (8) we have reverted to using \mathbf{B} in place of \mathbf{b} (recall that $\mathbf{B} = \mathbf{b}(4\pi\rho_0)^{1/2}$). Ψ is the electric potential. In deriving the invariance of H_m it is not necessary to use the Coulomb gauge. Equations (1) and (8) may be used to express the time rate of change of H_m in several ways. In particular we can write

$$\begin{aligned} \frac{dH_m}{dt} &= \int dS \hat{n} \cdot [-\mathbf{v} (\mathbf{A} \cdot \mathbf{B}) + \mathbf{B} (\mathbf{A} \cdot \mathbf{v} - \Psi)] \\ &= \int dS \hat{n} \cdot [-\mathbf{v} (\mathbf{A} \cdot \mathbf{B}) + \mathbf{B} (\mathbf{A} \cdot \mathbf{v}) - \mathbf{A} \times \nabla \Psi] \\ &= - \int dS \hat{n} \cdot [\mathbf{A} \times \partial \mathbf{A} / \partial t] - 2 \int dS (\hat{n} \cdot \mathbf{B}) \Psi \end{aligned}$$

The first of these indicates that $dH_m/dt = 0$ if $\hat{n} \cdot \mathbf{v} = \hat{n} \cdot \mathbf{B} = 0$ on S . From the second form it is evident that if the tangential component of the electrostatic field $-\nabla \Psi$ vanishes on S , then either $\mathbf{B} = 0$ or $\mathbf{v} = 0$ guarantees that H_m is an invariant. Periodic boundary conditions imposed on \mathbf{A} , Ψ , \mathbf{v} , and \mathbf{B} also lead to the invariance of H_m . The invariance of H_m was originally shown by Woltjer [1958a], who used the last of these three forms to argue that, in the gauge $\Psi = 0$, $\partial \mathbf{A} / \partial t$ vanishes on S for an isolated system and so, therefore, does dH_m/dt .

Before continuing, we digress for a moment to explore one of the subtleties involved in assuming periodic boundary conditions. Suppose that a turbulent fluid may be adequately described in terms of the properties of a single-fluid parcel of size L which is large enough to include a statistically representative sample of the fluid's behavior. This is generally justified if the size of this parcel is both much greater than the correlation length of the fluctuations and greater than any other relevant measures of the size of the dominant 'eddies.' If the physical system is sufficiently large and sufficiently smoothly varying so that one can consider any parcel of size L as being representative, then the model system is 'spatially homogeneous' [Batchelor, 1970]. In subsequent sections the notion of homogeneity will be discussed in greater detail. However, this qualitative definition of homogeneity will suffice for now to describe one of the difficulties in treating homogeneous MHD fluids with periodic boundary conditions. This difficulty has no analogue in ordinary hydrodynamic turbulence.

The complication arises when one adds a mean velocity \mathbf{V}_0 and a mean magnetic field \mathbf{B}_0 to a medium containing homogeneous fluctuations $\delta \mathbf{B}$ and $\delta \mathbf{v}$. It is clear that a mean flow \mathbf{V}_0 has no impact on the MHD model because a Galilean transformation can be found which removes it [Elsasser, 1956]. But the same cannot be said for the mean magnetic field \mathbf{B}_0 . In fact, \mathbf{B}_0 is responsible for new dynamical effects

including the propagation and scattering of large-amplitude Alfvén waves [Kraichnan, 1965]. What is the effect of adding \mathbf{B}_0 on the preservation of the three invariants of ideal MHD?

The first thing to note is that a uniform field \mathbf{B}_0 is itself periodic and so has no effect on the invariance of either H_c or E . The problem arises because the vector potential \mathbf{A}_0 which produces \mathbf{B}_0 is not periodic. Therefore we must reexamine the invariance of H_m . (We are indebted to L. Turner and D. Montgomery for valuable discussions on this issue.)

Equations (1), (7), and (8) together with the definitions $\mathbf{B} = \mathbf{B}_0 + \delta \mathbf{B}$ and $\mathbf{A} = \mathbf{A}_0 + \delta \mathbf{A}$ (where $\delta \mathbf{B} = \nabla \times \delta \mathbf{A}$), can be used to show that

$$\frac{dH_m'}{dt} = -2 \frac{d}{dt} (\mathbf{B}_0 \cdot \langle \mathbf{A} \rangle)$$

where $H_m' = (1/L^3) \int d^3x \delta \mathbf{B} \cdot \delta \mathbf{A}$ and $d(\mathbf{B}_0 \cdot \langle \mathbf{A} \rangle)/dt = (1/L^3) \mathbf{B}_0 \cdot \int d^3x \delta \mathbf{v} \times \delta \mathbf{B} = -\mathbf{B}_0 \cdot \langle \mathbf{E} \rangle$. We have assumed in this derivation that everything except \mathbf{A}_0 is periodic and no particular gauge need be chosen. $\langle \mathbf{E} \rangle$ is the volume average of the fluctuating electric field.

The new ideal invariant is neither H_m' nor H_m , but instead becomes $H_m' + 2\mathbf{B}_0 \cdot \langle \mathbf{A} \rangle$. Note that although by assuming a periodic model one has eliminated fluctuations with wavelength larger than the periodic box size L , the form of this 'new' magnetic helicity invariant includes what appear to be contributions from structures larger than L . The mean electric field $\langle \mathbf{E} \rangle$ produces correlations between the mean magnetic field \mathbf{B}_0 and the vector potential $\langle \mathbf{A} \rangle$, suggesting that topological linkages are produced by scales much larger than L [Moffatt, 1978].

For the present, this complication will be set aside and we shall assume that the 'fluctuating helicity' H_m is the quantity of theoretical interest, though it may not be conserved in the models which are periodic with a mean magnetic field.

The Physical Meaning of H_m

While the physical relevance of both the energy and cross helicity are clear enough, it may be worthwhile to discuss some physical aspects of the magnetic helicity. To do this, we return to the Coulomb gauge. This convention is important when dealing with model geometries for which \mathbf{B} does not vanish at large distances in one or more spatial directions. For isolated systems for which $\mathbf{B}(\mathbf{x}) \rightarrow 0$ as $|\mathbf{x}| \rightarrow \infty$, H_m is gauge invariant, as can be readily seen by adding a gradient of an arbitrary scalar to \mathbf{A} in (7) and integrating the gauge term by parts. H_m is also measurable for suitably bounded systems as well as for periodic systems with no mean magnetic field because \mathbf{A} is completely determined by values of $\nabla \times \mathbf{A} = \mathbf{B}$ within the system if appropriate boundary data are given [Panofsky and Phillips, 1962]. Explicit formulas for H_m have been given by Turner and Christiansen [1981]. From this point of view, the value of H_m would appear to depend on knowledge of $\mathbf{B}(\mathbf{x})$ at all \mathbf{x} in D . In section 3 we show that H_m can be evaluated in homogeneous turbulence without such global information.

An important property to notice about the magnetic helicity is that it is a pseudoscalar and changes sign under coordinate inversion $\mathbf{x} \rightarrow -\mathbf{x}$. Thus it is a measure of the lack of mirror symmetry of the magnetic field. More specifically, H_m is a measure of the topological linkage or 'knottedness' of magnetic field lines. An excellent discussion has been given by Moffatt [1978].

Nonvanishing H_m may also be viewed as a measure of the polarization of wavelike magnetic fields. Following Moffatt, one can compute the magnetic helicity of a circularly polarized magnetic field in slab geometry:

$$\mathbf{B}(z) = B(x \pm iy) e^{ikz - i\omega t}$$

The plus or minus sign corresponds to right or left circular polarization, respectively, for the case that both k and ω are positive. This field pattern is nonmirror symmetric and is maximally helical in the following sense. In the Coulomb gauge, $\mathbf{A} = \pm \mathbf{B}/k$, so that the spatially uniform helicity density is $\mathbf{A} \cdot \mathbf{B} = \pm B^2/k$. This is greater in absolute magnitude than is $\mathbf{A} \cdot \mathbf{B}$ in any mixed polarization wave with the same wave number and energy. In fact, for a single-slab wave of arbitrary polarization, $\sigma(k) \equiv k\mathbf{A} \cdot \mathbf{B}/B^2$ lies between -1 and $+1$ and is a useful normalized measure of the magnetic helicity in a single-wave mode.

It is also of interest to notice that a circularly polarized (maximal H_m) wave is 'force-free' [Woltjer, 1958a] in that the current density $\mathbf{j} = (c/4\pi)\nabla \times \mathbf{B} = (c/4\pi)k\mathbf{B}$. In fact, any field for which $\nabla \times \mathbf{A} = \lambda\mathbf{A}$ is also force free in the sense that $\mathbf{j} \propto \mathbf{B}$. While all force-free fields are not necessarily of maximal helicity, it has been suggested (D. Montgomery, private communication, 1981) that fields with $H_m \neq 0$ may typically be associated with situations in which currents are made to flow along a magnetic field, giving rise to helical field lines.

Rugged Invariants in MHD Turbulence

Investigation of the Fourier transform of the equations of motion (1)–(4) in either unbounded or periodic domains indicates that the nonlinear terms are entirely responsible for transferring energy from one length scale to another. Although viscous and Ohmic dissipation do not contribute to transfer between scales, they do serve preferentially to damp short wavelength fluctuations. The invariants of ideal MHD restrict the action of the nonlinear coupling at any instant of time, even in a nonideal magnetofluid. However, ideal MHD admits an uncountably infinite number of invariants. Most of these are associated with pointwise conservation laws. For example, the 'Alfvén flux invariants' [Cowling, 1976] guarantee that magnetic field lines are 'frozen-in.'

There are several reasons for not treating all ideal invariants on an equal footing. The most important is that many 'invariants' are preserved in time only for fluid models containing arbitrarily small spatial scales. Such invariants are of little interest if only because in both MHD and hydrodynamics this can never be true; there is always some scale size (ion gyroradius, interatomic spacing, Debye length, etc.) at which the fluid approximation breaks down. Even apart from this limitation, the solutions to the continuum ideal equations generally have only limited correspondence to physically observed turbulence. Ideal fluid models usually display a strong tendency to produce arbitrarily small spatial structures, perhaps to the extent of admitting infinite derivatives in finite time (see, for example, Morf *et al.* [1980]). On the other hand, all physical fluids and magnetofluids permit some dissipation, which, however weak, enforces a lower limit to the spatial scales that may appear in dynamical solutions. A properly formulated ideal model, however, can afford considerable insight into the behavior of a turbulent fluid. Thus it is important to select

from the large number of invariants of the ideal equations those that are meaningful in describing physical systems.

Kraichnan [1967] has introduced a technique to accomplish this. It consists of truncating the fluid equations at some minimum and maximum scale size. In Fourier space this corresponds to truncating the phase space of Fourier coefficients of (1)–(4) by considering only wave numbers k whose length lies between a minimum and maximum wave number. The properties of the ideal model thought to describe physical fluids are then recovered by taking the limit as the cutoff wave number increases. There is an extensive literature which utilizes this point of view, and the interested reader is referred to Kraichnan and Montgomery [1980] for more information. We note here that the 'rugged' ideal invariants are those which survive such a length scale truncation. A 'rugged' invariant is one that is a constant of the motion for a finite dimensional phase space ideal fluid model, as well as for the continuum ideal model.

The magnetic helicity, cross helicity, and energy are the only known rugged invariants of three-dimensional incompressible MHD [Frisch *et al.*, 1975]. All three of these simultaneously constrain nonlinear turbulent processes in MHD. Inverse cascade [Frisch *et al.*, 1975] and selective decay [Matthaeus and Montgomery, 1980; Montgomery *et al.*, 1978] hypotheses are examples of attempts to understand the roles of E , H_c , and H_m in nonideal MHD turbulence. Both the inverse cascade and selective decay hypotheses suggest that nonlinear turbulent MHD acts preferentially to transfer magnetic helicity to the slowly decaying largest scales in the system. Energy, on the other hand, is transferred predominantly to the small scales and is thus rapidly dissipated. As originally formulated, these hypotheses make no clear predictions concerning the behavior of cross helicity.

Alfvén Effect

The 'Alfvén effect' [Kraichnan, 1965] is the prediction that at wave numbers large in comparison with those characterizing the energy-containing scales, the magnetic energy per unit wave number should on average equal the kinetic energy per unit wave number. Fyfe and Montgomery [1977] have given a very simple justification for this conjecture and have verified it numerically in two dimensions. At the small scales, the energy per unit wave number (magnetic or kinetic) is generally smaller than it is at the energy-containing scales. The linear couplings of these small-scale modes with the energetic modes act to give equal amounts of magnetic and kinetic energy in each inertial range wave number interval, because the linear couplings are essentially Alfvén waves with equal time averaged kinetic and magnetic energies. In turbulence there are also nonlinear couplings among the small-scale modes, and these in general prevent the Alfvén waves from propagating far before undergoing substantial scattering. However the 'Alfvén effect' has been predicted to appear even in the presence of nonlinear interactions [Kraichnan, 1965; Fyfe and Montgomery, 1976].

A relatively simple physical picture can be given for this approximate equipartition in energy even in the presence of nonlinear interactions in magnetofluids with a mean field B_0 . As is well known (see, for example, Walén [1944], Kraichnan [1965], Goldstein *et al.* [1974], and Dobrowolny *et al.* [1980a]), the incompressible MHD equations permit Alfvénic solutions of arbitrary amplitude of the form $\delta\mathbf{v} = \pm\delta\mathbf{B}/$

$(4\pi\rho_0)^{1/2}$. Consider any fluctuation $\delta\mathbf{v}$, that has associated with it a zero fluctuation in \mathbf{B} . One can think of this as an initial condition for two Alfvénic wave packets, one with magnetic fluctuation $+\delta\mathbf{B}/(4\pi\rho_0)^{1/2}$ and the second with fluctuation $-\delta\mathbf{B}/(4\pi\rho_0)^{1/2}$. Thus assuming that the packets will propagate away from each other [Moffatt, 1978; Parker, 1979] with a speed of $B_0/(4\pi\rho_0)^{1/2}$, approximate equipartition of energy between magnetic and kinetic fluctuations is produced.

3. SPECTRA OF THE INVARIANTS IN HOMOGENEOUS TURBULENCE

Fourier decomposition of the energy, magnetic helicity, and cross helicity presupposes that the data represent either periodic or homogeneous fluctuations. This is the basic assumption in our analysis, and we discuss its justification further in section 4. Strict conditions for homogeneity cannot be met in the solar wind or, for that matter, in any finite system, and we can do no more than argue that the assumption of homogeneity is plausible and affords a valid approximation so long as certain length scale inequalities are fulfilled.

Statistical information about the state of a turbulent fluid is contained in the n -point correlation functions of the fluctuating fields [Batchelor, 1970]. In homogeneous turbulence these correlations are invariant under arbitrary translations of the experimental apparatus [G. I. Taylor, 1935]. For our purposes, the most important quantities are the one- and two-point correlation functions of the magnetic and fluid velocity fields. For the magnetic field we define $\mathbf{B}_0 \equiv \langle \mathbf{B}(\mathbf{x}) \rangle$ and

$$R_{ij}(\mathbf{r}) = \langle B_i(\mathbf{x}) B_j(\mathbf{x} + \mathbf{r}) \rangle \quad (9)$$

The fact that both B_{0i} and R_{ij} are independent of \mathbf{x} is a statement of 'weak' homogeneity. This is all that we require and we shall not impose restrictions on higher-order multi-point correlations. The brackets denote some form of ensemble averaging required to render the estimates statistically valid. Following standard practice, we shall routinely consider the two-point correlation R_{ij} to be constructed from the zero mean field so that $\mathbf{B} \rightarrow \mathbf{B} - \mathbf{B}_0$ is implied above. It is also straightforward to extend the above definition of R_{ij} to the case of two-time measurements as we shall do in the next section.

The two-point velocity correlation is similarly defined as

$$R_{ij}^v(\mathbf{r}) \equiv \langle v_i(\mathbf{x}) v_j(\mathbf{x} + \mathbf{r}) \rangle \quad (10)$$

while the cross helicity requires evaluation of the symmetric cross correlation

$$R_{ij}^{vB}(\mathbf{r}) \equiv (1/2) \langle v_i(\mathbf{x}) b_j(\mathbf{x} + \mathbf{r}) + b_i(\mathbf{x}) v_j(\mathbf{x} + \mathbf{r}) \rangle \quad (11)$$

Defined in this way R_{ij} , R_{ij}^v , and R_{ij}^{vB} have similar formal properties and they are all random homogeneous functions of fluctuating solenoidal fields. The homogeneity property implies that $R_{ij}(\mathbf{r}) = R_{ji}(-\mathbf{r})$ while the solenoidal condition $\nabla \cdot \mathbf{B} = 0$ and $\nabla \cdot \mathbf{v} = 0$ results in

$$\frac{\partial}{\partial r_i} R_{ij}(\mathbf{r}) = \frac{\partial}{\partial r_j} R_{ij}(\mathbf{r}) = 0$$

where R_{ij} can stand for any of the three correlation matrices defined above and summation over repeated indices is implied.

If one further assumes that the statistics of the fluctuations have a specific symmetry, it is then often possible to construct explicit analytical representations of R_{ij} . The technique for constructing R_{ij} from its symmetries is called the theory of isotropic tensors [Robertson, 1940; Batchelor, 1970]. The theory has been used to describe the form of R_{ij} when the fluctuations are either isotropic or axisymmetric about a mean flow direction \mathbf{V}_0 [Chandrasekhar, 1951] and, more recently, for the case of axisymmetric fluctuations about a mean magnetic field by Matthaeus and Smith [1981]. It will not be necessary for us to assume any specific symmetry with respect to either \mathbf{B}_0 or \mathbf{V}_0 . The solenoidal constraint and homogeneity will suffice.

We can now define the spectral tensors in terms of Fourier transforms of R_{ij} , R_{ij}^v , and R_{ij}^{vB} . Thus

$$R_{ij}(\mathbf{r}) = \int d^3k S_{ij}(\mathbf{k}) e^{i\mathbf{k} \cdot \mathbf{r}} \quad (12a)$$

$$R_{ij}^v(\mathbf{r}) = \int d^3k S_{ij}^v(\mathbf{k}) e^{i\mathbf{k} \cdot \mathbf{r}} \quad (12b)$$

and

$$R_{ij}^{vB}(\mathbf{r}) = \int d^3k S_{ij}^{vB}(\mathbf{k}) e^{i\mathbf{k} \cdot \mathbf{r}} \quad (12c)$$

We will call S_{ij} the energy spectrum tensor, S_{ij}^v the kinetic energy spectrum tensor, and S_{ij}^{vB} the cross-helicity spectrum tensor [Frisch *et al.*, 1975; Batchelor, 1970].

Some subtlety is involved in applying the homogeneity model to physical systems because $R_{ij} \rightarrow 0$ at large separations is a necessary condition for spectra to exist [Cramér, 1940], whereas homogeneity requires that \mathbf{B} have the same statistical properties everywhere so that the fluctuations $\delta\mathbf{B}$ do not vanish at infinity. These are difficulties that have been resolved in the classic hydrodynamic turbulence literature (see, for example, Batchelor [1970], Panchev [1971], and Appendix B).

The spectral decomposition of energy and cross helicity may be accomplished using (5), (6), and (12), giving

$$E = \int d^3k [E_v(\mathbf{k}) + E_B(\mathbf{k})] \quad (13)$$

and

$$H_c = \int d^3k H_c(\mathbf{k}) \quad (14)$$

In (13) the kinetic energy spectrum $E_v(\mathbf{k}) \equiv \text{trace } S^v(\mathbf{k})$, the magnetic energy spectrum $E_B(\mathbf{k}) \equiv \text{trace } S(\mathbf{k})$, and the cross-helicity spectrum $H_c(\mathbf{k}) \equiv \text{trace } S^{vB}(\mathbf{k})$. These results follow directly since from (9)–(11) the kinetic energy (per unit mass) $E_v \equiv \text{trace } R^v(0)$, the magnetic energy (per unit mass) $E_B \equiv \text{trace } R(0)$, and the cross helicity (per unit mass) $H_c \equiv \text{trace } R^{vB}(0)$. Note that, for convenience, we drop the factor of 1/2 in the definitions (5) and (6).

What are generally available in space experiments are data from only a single spacecraft. This provides values of R , R^v , and R^{vB} for collinear sequences of separations \mathbf{r} . In this situation a full Fourier decomposition is not possible [Batchelor, 1970], but reduced (one dimensional) spectra are available. Specifically, for the magnetic field, we may determine $R_{ij}(r_1, 0, 0)$ where \mathbf{e}_1 is the direction of collinear separations. The Fourier transform on r_1 yields the reduced spectrum tensor S'

$$\begin{aligned} S'_{ij}(k_1) &= (1/2\pi) \int dr_1 e^{-ik_1 r_1} R_{ij}(r_1, 0, 0) \\ &= \int dk_2 dk_3 S_{ij}(k_1, k_2, k_3) \end{aligned} \quad (15)$$

The last line indicates that S'_{ij} may be obtained from the full

tensor S by integrating over transverse wave numbers. We define H_m^r , H_c^r , and $E^r = E_v^r + E_B^r$ as the reduced spectra of the invariants, depending only on wave number k_1 .

In most cases, information about S_{ij} is lost in 'reducing' it to S_{ij}^r . However, for slab [Jokipii, 1966] and isotropic [Batchelor, 1970] symmetries the reduced spectral tensor contains all the information of the full tensor. In slab geometry (see section 2), $\mathbf{k} = \hat{\mathbf{e}}_1 k_1$ and $\hat{\mathbf{e}}_1 \cdot \mathbf{S} \cdot \hat{\mathbf{e}}_1 = 0$. This is equivalent to noting that the spectral tensor $S \propto \delta(k_2)\delta(k_3)$ and no functional dependence is lost by performing the transverse wave number integrals in (15). Isotropic symmetry is usually treated in terms of an omnidirectional energy spectrum, $\tilde{E}(k) = 4\pi k^2 E(k)$, with scalar argument $k = |\mathbf{k}|$, such that $E = \int dk \tilde{E}(k)$. It is well known that [Batchelor, 1970]

$$\tilde{E}(k) = k_1 \left\{ \frac{d}{dk_1} \left[\frac{1}{k_1} \frac{d}{dk_1} E^r(k_1) \right] \right\} \Big|_{k_1=k}$$

where $E^r(k_1) \equiv S_{ii}^r(k_1)$. It is clear that the full spectral wave number dependence is retained. A corollary is that reduced spectra of the form $E(k) \propto k^{-\alpha}$ may equally well be thought of as isotropic or slab spectra with the same spectral index α . In the general case of unspecified rotational symmetry there is no connection between reduced and full spectra [Jokipii, 1966; Fredricks and Coroniti, 1976]. If the correlations have axisymmetric symmetry [Matthaeus and Smith, 1981], no manipulation of the one-dimensional spectrum has been found that allows extraction of scalar functions which describe the distribution of energy as a function of angle and modulus of the magnitude of the wave number.

While power spectra of the magnetic field and, to a lesser extent, the cross helicity have been obtained for many years (see, for example, Jokipii and Coleman [1968], Coleman [1966, 1967, 1968], Sari and Ness [1969], and Belcher and Davis [1971]), only recently has it been recognized that the magnetic helicity is equally measurable in homogeneous turbulence [Matthaeus et al., 1982]. Although the magnetic helicity has not been utilized in the past in describing properties of interplanetary fluctuations, it has been of recurrent interest in theoretical plasma physics (see, for example, Woltjer [1958a, b], J. B. Taylor [1974], Frisch et al. [1975], Matthaeus and Montgomery [1980], and Chu [1982]). Because the measurement of the magnetic helicity in the solar wind is one of the new and central results of this paper, we describe below in some detail the theoretical basis of these measurements.

Begin by noting that R and S may always be decomposed into symmetric and antisymmetric parts. Therefore we write $R = R^s + R^a$ where $R_{ij}^s = R_{ji}^s$ and $R_{ij}^a = -R_{ji}^a$. Now consider the action of the coordinate inversion operator I on R^s and R^a separately. (Recall that $I\mathbf{r} = -\mathbf{r}$ whereas $I\mathbf{B} = \mathbf{B}$ because magnetic fields are 'pseudovectors'.) Because R^s is symmetric in its indices, homogeneity ($R_{ij}^s(\mathbf{r}) = R_{ji}^s(-\mathbf{r})$) implies that $IR^s = R^s$. Similarly because homogeneity requires that $R^a(\mathbf{r}) = -R^a(-\mathbf{r})$, it follows that $IR^a = -R^a$.

Thus R^s is a 'proper' second rank tensor and R^a is a second-rank 'pseudotensor.' The argument may be inverted to show that any homogeneous second-rank pseudotensor must be antisymmetric in its indices and any second-rank homogeneous proper tensor must be symmetric in its indices. We conclude that homogeneous correlation matrices consist of the sum of a proper tensor, symmetric in its

indices and even in its spatial argument, and a pseudotensor, antisymmetric in its indices and odd in its spatial argument. All of these statements apply equally well in Fourier space to the decomposition of the spectral matrix $S_{ij}(\mathbf{k})$, but with parity in \mathbf{k} replacing parity in \mathbf{r} . Since these statements are true for any homogeneous autocorrelation function and spectral matrix, we identify R_{ij} and S_{ij} with the definitions (9) and (12a). We turn now to the problem of extracting information about H_m from $R_{ij}(\mathbf{r})$.

First note that the relevant part of the $\langle AB \rangle$ correlation may be obtained from $S_{ij}(\mathbf{k})$ by 'uncurling' in Fourier space [Montgomery and Turner, 1981]. If the symmetric part of the Fourier transform of $\langle AB \rangle$ is denoted by $H_{ij}(\mathbf{k})$, we have

$$H_{ij}(\mathbf{k}) = i\epsilon_{ilm}k_l S_{mj}(\mathbf{k})/k^2 \quad (16)$$

The spectral decomposition of H_m is $H_m(\mathbf{k}) = H_{ii}(\mathbf{k}) = \text{trace } H_{ij}(\mathbf{k})$. It is also clear that H_{ij} depends only on the antisymmetric (pseudotensor) part of S_{ij} , because $\epsilon_{ilm}k_l S_{mi}^s = 0$ for any symmetric matrix S^s .

It only remains to prove that S^a has a unique form simple enough to determine the reduced spectrum of H_m . Even in the most general homogeneous case it is possible to enumerate all the tensor forms that may additively contribute to S . These may be constructed as was done by Batchelor [1970] from the theory of isotropic tensors by considering all two-indexed objects composed of either the wave vector \mathbf{k} , the Levi Civita symbol ϵ_{ijk} , the Kronecker matrix δ_{ij} , or the two-unit vectors corresponding to the two independent principal axes of the energy spectrum tensor. Batchelor found 31 such forms. Restricting ourselves to combinations that are explicitly antisymmetric in indices and using the solenoidal constraint, it is straightforward to show that the only independent antisymmetric form is $\epsilon_{ijk}k_l$. The same result can be obtained using a polarization basis set as defined by Montgomery and Turner [1981].

If we let $G(\mathbf{k})$ be any even function of \mathbf{k} and insert $S_{ij}^a = \epsilon_{ijk}k_l G(\mathbf{k})$ into (16), it follows that $G(\mathbf{k}) = iH(\mathbf{k})/2$. Therefore the spectrum of H_m explicitly appears in the magnetic energy spectrum tensor in the form

$$S_{ij}(\mathbf{k}) - S_{ji}(\mathbf{k}) = i\epsilon_{ijk}k_l H_m(\mathbf{k})$$

In configuration space this corresponds to $R_{ij}^a(\mathbf{r}) = \epsilon_{ijk}\partial\Phi(\mathbf{r})/\partial r_k$, where Φ is an even function of \mathbf{r} and $2\Phi(0) = \langle \mathbf{A} \cdot \mathbf{B} \rangle = H_m$. The Fourier transform of Φ is $H_m(\mathbf{k})/2$.

The simple connection between the total magnetic helicity density and the single scalar function Φ which generates the antisymmetric part of the correlation matrix (namely, $2\Phi(0) = H_m$) allows us to write

$$H_m = - \int_0^\infty dr_1 [R_{23}(r_1, 0, 0) - R_{32}(r_1, 0, 0)] \quad (17)$$

This result also follows for any cyclic permutation of the three indices contained in the integral. Because the dimensions of H_m and E differ by a length, the ratio

$$\lambda_H = H_m/E \quad (18)$$

is a natural measure of the scale over which the antisymmetric correlations vanish. It will be seen in section 4 that λ_H has a structure similar to the correlation length and may be thought of as a 'helicity correlation length.'

As was the case for the energy spectrum, a reduced helicity spectrum can be obtained from R_{ij} when separations

are available only in one direction. Let \hat{e}_1 again be the direction in which the collinear separations $R_{ij}(r_1, 0, 0)$ are known. If we note that S is Hermitian (because it is the Fourier transform of a real, homogeneous matrix) then it is clear that the only imaginary part of S is the antisymmetric pseudotensor, so that

$$\int dk_2 dk_3 \operatorname{Im} S_{23}(\mathbf{k}) = (k_1/2) \int dk_2 dk_3 H_m(\mathbf{k})$$

or

$$H_m'(k_1) = 2 \operatorname{Im} S_{23}'(k_1)/k_1 \quad (19)$$

This defines the reduced magnetic helicity spectrum. Equation (19) is the basic equation used in constructing magnetic helicity spectra in sections 4 and 5.

The magnetic helicity computed by this technique is only that which arises from the homogeneous fluctuations of \mathbf{B} . The magnetic helicity of any 'mean field' structures on the scale of the inhomogeneities of the system is not resolved by this approach.

4. THE MEASUREMENT OF ENERGY, CROSS-HELICITY, AND MAGNETIC HELICITY SPECTRA

In this section we first discuss the validity of the usual correspondence between frequency and wave number spectra made when analyzing MHD fluctuations in the solar wind. We then redefine the invariants in a manner more appropriate for analysis of homogeneous systems. A discussion of the problem of trend removal and the relative merits of the Blackman-Tukey and fast Fourier transform techniques completes this section. Readers who feel familiar with these issues may wish to proceed directly to section 5, where the results are presented.

The 'Frozen-in' Approximation

Voyager magnetic field and plasma experiments [Behannon *et al.*, 1977; Bridge *et al.*, 1977] provide time series of \mathbf{B} and \mathbf{v} , respectively. The correlations constructed from those series are essentially two-time single-point measurements. The frequency decompositions of \mathbf{v} and \mathbf{B} at the spacecraft's location are usually interpreted as wave number decompositions because the mean solar wind speed is super-Alfvénic and the measured frequencies are less than the Doppler-shifted proton cyclotron frequency. Some simple arguments can be given to justify this assumption in terms of MHD turbulence theory. We first extend the definition of the correlation matrix to include temporal as well as spatial separations in a homogeneous and stationary system by rewriting the correlation matrix as

$$R_{ij}(\mathbf{r}, t) = \langle B_i(\mathbf{x}, \tau) B_j(\mathbf{x} + \mathbf{r}, \tau + t) \rangle$$

Denoting the solar wind velocity as $V_{sw}\hat{\mathbf{R}}$ (where $\hat{\mathbf{R}}$ is a unit vector in the heliocentric radial direction), we investigate the claim that $R_{ij}(V_{sw}\hat{\mathbf{R}}t, 0) = R_{ij}(0, -t)$. When this holds, the relation $\omega = V_{sw}k$ can be used to relate frequency spectra to wave number spectra. These approximations are the MHD analogues of the Taylor 'frozen-in flow' hypothesis [G. I. Taylor, 1938].

It is reasonable to suppose that fluctuations are 'frozen in' in the above sense if a 'magnetic eddy' of size $\lambda = 2\pi/k$ transits the spacecraft in a time t which is small in comparison with the characteristic time t_λ for dynamical evolution of structures of size λ . On average, magnetic eddies are con-

vected outward with speed V_{sw} so that $t \approx \lambda/V_{sw}$. The most stringent condition is obtained for the case of fluctuations which are propagating Alfvén waves so that $t_\lambda = \lambda/b_0$, where b_0 is the large-scale ('mean') magnetic field in Alfvén speed units. The $t_\lambda \gg t$ only if $V_{sw} \gg b_0$, which is usually well satisfied.

If the fluctuations represent fully developed turbulence, this condition is somewhat relaxed. Eddy turnover times for turbulent magnetic structures may be estimated [Batchelor, 1970] as $t_\lambda \approx 1/(b_k k)$, where b_k is the Fourier series amplitude at wave number k measured in units of speed as defined in section 2. The condition $t_\lambda \gg t$ will be satisfied if

$$V_{sw} \gg 2\pi b_k \quad (20)$$

This simple relation may be interpreted in several ways. First, b_k may be thought of as the propagation speed of infinitesimal waves with wave number much greater than $2\pi/\lambda$ propagating in a medium whose mean magnetic field is $|b_k|$. An alternative interpretation is obtained by rewriting (20) as

$$V_{sw}/V_A \gg 2\pi(\delta B/B) \quad (21)$$

where V_A is the Alfvén speed in the rms field B , and δB symbolically represents the rms magnetic field contribution of the magnetic eddy in question. The left-hand side of this inequality is typically of order 10 in the solar wind. The magnitude of δB depends on k , but for the large-scale structures that contain the most energy, $\delta B/B \approx 1/2$, while for smaller structures $\delta B/B \ll 1$ [Chang and Nishida, 1973; Burlaga and Turner, 1976]. Thus (20) or (21) is usually satisfied in the solar wind by a large factor and 'frozen-in flux' is a valid approximation.

The eddy turnover time t_λ could have been estimated equally well in terms of v_k , the rms value of the velocity field at size $2\pi/k$. However, because of the 'Alfvén effect' (section 2), for small eddies $v_k \approx b_k$ and (20) or (21) is still well satisfied. One can similarly conclude that velocity fluctuations are frozen in. Consequently, we shall assume that the 'frozen-in' approximation holds for all MHD scale fluctuations in the solar wind.

Redefinition of the Invariants

When one considers homogeneous turbulence, it is customary to redefine the invariants E , H_m , and H_c as their 'per unit volume' values by introducing a factor of $1/(\text{volume})$ in the right-hand sides of (5), (6), and (7). The invariants are now the ensemble averaged quantities $E = \langle v^2 + b^2 \rangle$, $H_c = \langle \mathbf{v} \cdot \mathbf{b} \rangle$, and $H_m = \langle \mathbf{A} \cdot \mathbf{B} \rangle$.

In section 4, E , H_m , and H_c are computed from measurements along a line in the $\hat{\mathbf{R}}$ direction. The length of this line is $2L = V_{sw}T$, where T is the duration of the data interval. Thus, for example, the definition of E becomes

$$E = (1/2L) \int_{-L}^L dx (v^2 + b^2)$$

H_c and H_m can be written similarly.

Fundamental Assumption

The fundamental assumption of our methods is that by choosing large enough data intervals L , the correlation function $R(r) \equiv \text{trace } R_{ij}(r)$ becomes a Lanczos-type function (see Appendix B) in that $R(r) \approx 0$ for $r \geq L_0$, where $L_0 < L$ is the maximum lag. Thus we require that our data sets satisfy

$R(L_0)/R(0) \ll 1$. We have found that this is generally true if $L > 5-10L_c$, where L_c is the correlation length defined as in the work of Batchelor [1970] to be

$$L_c = \int_0^\infty dr R(r)/R(0) \quad (22)$$

If R is of the Lanczos type, the Fourier series and Fourier integral spectral tensors are related by (B1). Furthermore, the distinction between a large periodic system and a homogeneous system becomes unimportant.

The fact that Lanczos-type correlation functions can be found in solar wind data (section 5) lends weight to the heuristic argument of section 3 that these fluctuations are homogeneous. Until more rigorous studies are available [Matthaeus and Goldstein, 1982], we will view this as sufficient justification for the assumption of homogeneity. Similar statements apply equally well to individual components of R_{ij} as well as to the analogous properties of R_{ij}^v and R_{ij}^{vB} .

We adopt the convention that the spectral matrices S_{ij} , S_{ij}^v , and S_{ij}^{vB} are the Fourier series amplitudes of their respective correlation matrices given, for example, by

$$S_{ij}(k) = (1/2L) \int_{-L}^L dr R_{ij}(r) e^{-ikr} \quad (23)$$

In practice the discrete version of (23) and its inverse are used, involving a finite number of equally spaced positions and wave numbers.

To ensure that $R(r) \rightarrow 0$ at large r , we have chosen data sets spanning several days corresponding to L of the order of a few AU. Such scales approach the inhomogeneity length of the system. We have also avoided use of data sets containing isolated interplanetary shocks or sector crossings, but other discontinuities are retained. The approximate homogeneity of the data is not affected by the large number of these discontinuities which are treated here as an intrinsic part of the turbulence.

Trend Removal

In the most elementary sense, a data record of length $2L$ can be said to have a trend if the values of $B_i(r \approx -L)$ systematically differ from $B_i(r \approx L)$ by, say, $\Delta B_i \neq 0$. Time series analysis techniques frequently include algorithms for detrending such data, for example, by subtracting an appropriate linear ('ramp') function. The justification for detrending is that the trend introduces spurious spectral power or, equivalently, that the trend inhibits $R(r)$ going to zero as $r \rightarrow L$.

We have chosen not to detrend our data records for several reasons. First, the total power subtracted by trend removal, using either a ramp or a discontinuity model of the trend, will be of the order of ΔB^2 . The trend contributes to the energy spectrum with a $1/k^2$ dependence. Thus it is basically a low k effect and does not affect small-scale power which generally falls off more slowly than $1/k^2$ in the MHD range. Detrending the data then reduces low-wave-number power in an ad hoc fashion. The undesirability of this is clear when contributions to the power at the longest wavelengths are of central importance. Investigation of the low k behavior of the invariants is of particular interest, but in addition, because of the requirement that the medium be homogeneous, we will be interested in the behavior of the correlation

length, which is also very sensitive to the long-wavelength power (see Appendix B). Detrending systematically reduces L_c which can cause the data record to appear more homogeneous than it is.

To conclude this section, we briefly review the two central techniques used to construct correlation functions and spectra. These are the Blackman-Tukey ('mean lagged product') and fast Fourier transform (FFT). In the remainder of this discussion we shall assume that all correlation matrices are functions only of the heliocentric radial coordinate, and the corresponding spectra are reduced.

Blackman-Tukey and Fast Fourier Transform Techniques

The Blackman-Tukey technique has been well studied [Blackman and Tukey, 1958; Otnes and Enochson, 1972] and often utilized in analyzing solar wind magnetic fluctuations (for example, Jokipii and Coleman [1968], Sari and Ness [1969], Behannon [1978], and Hedgecock [1975], among many others). Consequently, we will not present a complete analysis of the approach here. The essence of the method is the computation of the correlation function $R_{ij}(r)$ by the formula

$$R_{ij}(n) = \frac{1}{M-n} \sum_{P=1}^{M-n} B_i(P) B_j(P+n) \quad (24)$$

$$n = 0, 1, 2, \dots, N$$

In this formula, N is the maximum lag for which R_{ij} is evaluated and M is the number of data values in the record. Data points are separated in space by Δx within the record. In (24), position is denoted by an integer where, for example, $R_{ij}(n) = R_{ij}(n\Delta x)$. The spectral matrix $S_{ij}(k)$ is then obtained from R_{ij} by taking a (fast) Fourier transform.

The principal advantage of the Blackman-Tukey technique is that R_{ij} is directly calculated and the goal that $R(r) \rightarrow 0$ for large r can be verified. To avoid any residual power 'leakage' [Hamming, 1973; Otnes and Enochson, 1972], the calculated $R_{ij}(r)$ is windowed (we commonly used a 10% cosine taper) and the values are padded with extra zeros from N (the length of the maximum separation) to M (the length of the interval). As a result, the resolution of the power spectrum is increased and a smooth interpolation of the information in the unpadded $R_{ij}(r)$ results which in turn allows easy comparison with a fast Fourier transform analysis of the same interval. The windowing step introduces only small changes in the calculated spectra provided that $R(N)/R(0) \ll 1$.

One important property of the Blackman-Tukey technique is that it does not guarantee positive definiteness of the energy spectrum unless $M - N \rightarrow \infty$ in (24). In practice, we have found that with $M/N = 10$ (20 degrees of freedom) and $M \approx \text{few} \times 10^3$, positive power spectra and adequate statistical validity can be obtained. Whenever feasible, data have been low pass filtered and decimated to eliminate high k aliasing [Hamming, 1973]. Small data gaps and any obviously bad data points are flagged and the corresponding lagged products in (24) are eliminated. The Blackman-Tukey technique is perhaps the most reliable method for calculating spectra, but it is unfortunately an extremely slow method when N and M are large. This leads us to the second technique which is much faster, but perhaps somewhat more perilous.

The fast Fourier transform technique is based on the relation

$$S_{ij}(k) = \langle B_i(-k)B_j(k) \rangle \quad (25)$$

where $B_i(k)$ is the Fourier series representation of the magnetic field $B_i(r)$. Equation (25) holds strictly only for periodic functions $B_i(r)$; there is also an analogous relation involving Fourier transforms which holds for homogeneous fluctuations [see Orszag, 1977].

The ensemble average denoted by the angle brackets in (25) is accomplished by performing a sliding P point average of $S_{ij}(k)$. Generally, $P \approx 13$ is adequate to obtain good agreement with the Blackman-Tukey results. Small data gaps and 'bad data points' are removed and filled with linearly interpolated points to supply the fast Fourier transform with contiguous data. Windowing of the data set is not performed for the same reasons given above for not detrending, namely, that interesting small wave number behavior would be undesirably modified. The computational advantage of the fast Fourier transform method is great enough that we have relied on it for most of our analysis. However, it must be used with care because (25) is valid only for homogeneous systems.

One potential disadvantage of using the fast Fourier transform technique is the possibility that 'leakage' [Otnes and Enochson, 1972] will distort the high-wave-number end of the spectrum. The magnetic helicity measurements are particularly sensitive to this problem. We have checked against such distortions of our analysis in several ways. First, by utilizing long data sets for which the correlation functions are approximately Lanczos type, leakage is minimized. Second, we have compared the fast Fourier transform results to those obtained from the Blackman-Tukey method in which leakage has been strictly eliminated by windowing the correlation function. As is shown in section 5, the agreement between the two methods is excellent and leakage is not a problem. A third test was to 'prewhiten' the magnetic field data by passing it through a differentiating filter [McClellan *et al.*, 1979]. The effect of this filter is to flatten the power spectrum and thus minimize any influence at high wave numbers of leakage from the low wave numbers. The magnetic helicity as measured by the polarization parameter σ (section 2 and (27), below) computed from the prewhitened time series was identical (except, of course, at the very lowest wave numbers) to that computed directly from the unfiltered data.

5. ANALYSIS OF VOYAGER DATA

The trajectories of the voyager 1 and 2 spacecraft cover an order of magnitude in heliocentric distance, which allows the possibility of examining the MHD evolution of the solar wind over a significant portion of the heliosphere. The instrumentation and data reduction routines have been designed to provide simultaneous three-dimensional velocity and magnetic field vectors. The completeness of this data set and the nearly continuous tracking of the Voyager spacecraft during a portion of the mission have enabled us to compute all components of the reduced cross helicity and energy spectral matrices. The merged data summary tape combining both the magnetometer and thermal plasma data has been an invaluable aid in the construction of the two invariants which require simultaneous measurement of the magnetic field and plasma parameters, and we are indebted to both the plasma

and magnetometer teams for their help in utilizing that data base.

The low-field magnetometer experiment (N. F. Ness, principal investigator) provides three orthogonal measurements of magnetic field intensity at a maximum sampling rate of $16\frac{2}{3}$ vector measurements per second with an absolute error of less than 0.1γ ($1 \gamma = 1$ nanotesla) [Behannon *et al.*, 1977]. In constructing power spectra of the magnetic fluctuations we have typically used either 9.6-s averages or 48-s averages of the data which were then digitally filtered using a low-pass filter to remove aliasing. The low-energy plasma spectrometer (H. Bridge, principal investigator) measures the three-dimensional phase space distributions of both ions and electrons. We have used only the ion velocity and density data (for protons and alpha particles) in this study. These data are typically obtained every 96 s during the cruise portion of the mission.

The techniques described in section 4 for measuring the three rugged invariants of ideal MHD have been used to analyze several time intervals. We present representative examples illustrating the techniques used but make no attempt here to give a comprehensive view of the evolution of the invariants throughout the 1–10 AU region that has been covered by the spacecraft. The properties of three intervals analyzed are summarized in Table 1. These intervals are similar to others we have investigated and appear to satisfy the requirements of homogeneity discussed in section 2. In the remainder of this section we discuss each of these intervals in some detail.

1 AU

This first interval contains data taken by Voyager 1 shortly after launch in 1977, but still well outside the influence of the earth's magnetosphere. This interval (from day 250 hour 9 to day 252 hour 1, September 7–9, 1977) is a subset of a larger interval (ending on day 254) that contained a sector crossing. During the period analyzed, however, the plasma has a relatively low velocity of 352 km/s (see Table 1). The results presented here utilized 9.6-s averaged magnetic field data that were digitally filtered using a 128-point low-pass Remez exchange algorithm [McClellan *et al.*, 1979] and then decimated by three to give a time spacing $\Delta t = 28.8$ s. Approximately 6% of this interval contained data gaps or bad data points.

The plasma data during this interval were obtained every 96 s and 11% of the data were either missing or bad. The mean density was 12.6 protons/cm³. Alpha particles made up approximately 5% of the total ion density at this time. The mean proton and alpha particle densities were included in transforming the magnetic field to velocity units.

Figure 1 shows the magnetic field correlation function (in units of γ^2) plotted against time and distance using the measured average solar wind speed of 352 km/s. More precisely, we have plotted $R(r) = \text{trace } R_{ij}(r)$ as calculated from the Blackman-Tukey technique. $R(r)$ decreases from a maximum value of $9.91 \gamma^2$ at zero separation (the fluctuating magnetic energy density) to less than $0.3 \gamma^2$ at the maximum lag of 5×10^6 km (one tenth the total interval length). The fact that $R(r)$ decreases to 3% of its peak value is strong evidence that R is a 'Lanczos-type' (cf. Appendix B) function and that the homogeneity assumption is satisfied.

In Figure 2 the Blackman-Tukey magnetic energy spectrum $E_B(k)$ (plotted as the thicker line) is compared with the

TABLE 1. Summary of Analysis

| Intervals | 1 AU | 2.8 AU | 5 AU |
|--|-----------------------|-----------------------|-----------------------|
| Begin time, year, day, time | 1977, 250, 0822 | | 1979, 6, 0051 |
| End time, year, day, time | 1977, 254, 2002 | | 1979, 10, 2222 |
| Mean solar wind speed, km/s | 352 | | 507 |
| Mean proton density, no./cm ³ | 12.6 | | 0.0497 |
| Fluctuating magnetic energy density, γ^2 | 9.91 | | 0.0272 |
| Magnetic helicity density, γ^2 km | 2.64×10^6 | | -1.15×10^4 |
| Total fluctuation energy per unit mass, (km/s) ² | 672.5 | | 2131 |
| Fluctuation kinetic energy per unit mass, (km/s) ² | 325.3 | 390.9 | 1845 |
| Fluctuation cross helicity, (km/s) ² | 16 | -160 | 233 |
| Magnetic correlation length L_c , cm | 1.12×10^{11} | 1.06×10^{12} | 1.62×10^{12} |
| Velocity correlation length, cm | 2.83×10^{11} | 1.30×10^{12} | 3.30×10^{12} |
| Magnetic helicity correlation length λ_H , cm | 1.7×10^{11} | 2.0×10^{12} | -2.6×10^{11} |
| Cross-helicity correlation length $\int dr R_{ii}^{vB}/H_c$, cm | 1.3×10^{12} | 5.5×10^{12} | 4.4×10^{12} |
| Magnetic 1-D Taylor micro-scale λ , cm | 3.18×10^{10} | 1.29×10^{11} | 2.20×10^{11} |
| Velocity 1-D Taylor micro-scale, cm | 6.08×10^{10} | 6.1×10^{10} | 1.9×10^{11} |
| $\lambda_{2H} = 2\pi H_m/(\sum k^2 H_c(k))^{1/2}$, cm | 1.2×10^{12} | 4.56×10^{12} | 6.18×10^{12} |
| $\lambda_{2Hc} = 2\pi H_c/(\sum k^2 H_c(k))^{1/2}$, cm | 6.4×10^9 | 3.8×10^{10} | 2.44×10^{11} |
| $\lambda_{1E} = 2\pi E_B/\sum k E_B(k)$, cm (equation (28b)) | 1.08×10^{11} | 3.44×10^{11} | 9.45×10^{11} |
| $\lambda_{1H} = 2\pi H_m/\sum k H_m(k)$, cm (equation (28a)) | 2.31×10^{12} | 1.19×10^{13} | 4.98×10^{12} |
| $\lambda_{1Hc} = 2\pi H_c/\sum k H_c(k)$, cm | 2.7×10^9 | 7.04×10^{10} | 4.4×10^{12} |

spectrum obtained using the fast Fourier transform technique (plotted as the thin line). The two spectra have been made comparable by 'smoothing' the fast Fourier transform spectrum with a 13-point moving centered average at all but the seven lowest and highest wave numbers. This 'ensemble average' of the fast Fourier transform spectrum gives it approximately the same statistical weight as that of the

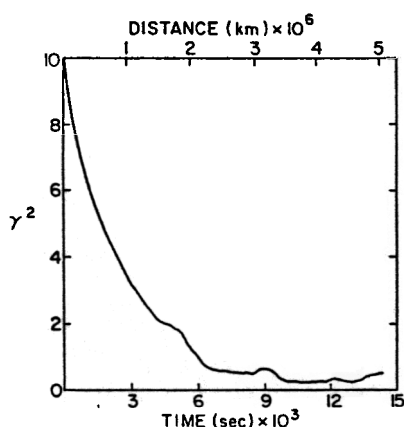


Fig. 1. The magnetic field correlation function $R(r)$ for the 1 AU interval, in units of γ^2 ($1 \gamma = 1$ nanotesla (nT)). The abscissa is given in both time and distance units. The largest-scale fluctuations represented are nearly uncorrelated.

Blackman-Tukey spectrum which has 20 degrees of freedom. The Blackman-Tukey version of $E_B(k)$ has been interpolated and extended to wave numbers as low as those in the fast Fourier transform by windowing and (trivially) extending the range of r by padding $R(r)$ with zeros from 5×10^{11} cm to L , the total data interval of 5×10^{12} cm. At the higher k 's, where both techniques have equal statistical weight, the spectra are essentially indistinguishable. At the lowest wave numbers there is also good agreement. This is itself remarkable because the first 10 Blackman-Tukey spectral estimates have built into them the assumption that the correlation function $R(r)$ vanishes for $r > 5 \times 10^{11}$ cm. What is seen at low k in the Blackman-Tukey plot is just the asymptotic behavior of the spectrum as described in Appendix B. This behavior is guaranteed by the Blackman-Tukey technique. No such assumptions are present in the fast Fourier transform technique. Despite the lack of statistical weight of the small k fast Fourier transform spectral estimates, their qualitative agreement with the small k Blackman-Tukey estimates appears to be further evidence that the observed fluctuations are very nearly homogeneous during this time.

The magnetic energy spectrum in Figure 2 displays a nearly power law behavior for some $2\frac{1}{2}$ decades in wave number between 10^{-11} /cm and 3×10^{-9} /cm. The spectral index is -1.73 ± 0.08 . At the low-wave-number end of the spectrum, the 'break' in the power law behavior signifies that uncorrelated fluctuations are being sampled, consistent with calculation of the correlation length (22), $L_c = 1.12 \times$

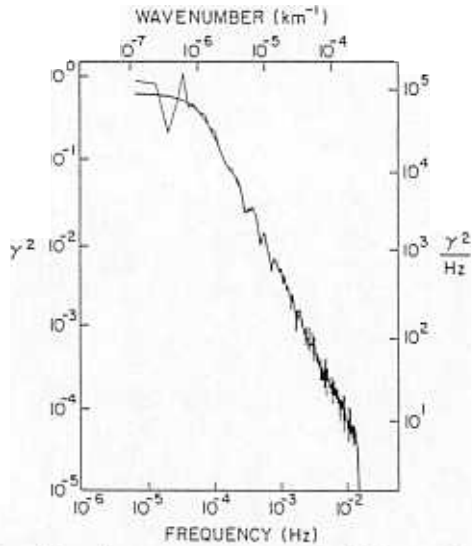


Fig. 2. Magnetic energy spectrum of 1 AU interval, in units of γ^2 . The abscissa is given in both frequency (Hz) and wave number (km^{-1}). The frequency spacing is 6.94×10^{-6} Hz. Wave number spacing is $1.24 \times 10^{-7} \text{ km}^{-1}$. The spectrum using the Blackman-Tukey algorithm is plotted as the thicker line. The fast Fourier transform results are plotted as the thin line.

10^{11} cm using the fast Fourier transform technique and about 10% less using the Blackman-Tukey algorithm.

Another length of interest is

$$\lambda \approx 2\pi \left(\sum_k k^2 E_B(k) / E_B \right)^{1/2} \quad (26)$$

This is the one-dimensional analogue of the Taylor micro-scale [Orszag, 1977; Batchelor, 1970] and characterizes the gradients of the magnetic field in the \hat{R} direction. In the isotropic case, λ typifies the size of electric current structures. For the spectra in Figure 2, $\lambda \approx 3.2 \times 10^{10}$ cm. The fact that $\lambda < L_c$ indicates that magnetic structures are spread over a fairly wide range of spatial scales. Because the spectrum in Figure 2 does not extend into the dissipation range, this value of λ is an upper bound.

The spectral decomposition of the total energy, $E(k) = E_B(k) + E_v(k)$ is shown in Figure 3. Again a power law dependence of the form $k^{-1.69 \pm 0.08}$ is seen at all but the lowest wave numbers. The similarity of the spectral shape of $E(k)$ in Figure 3 to that of $E_B(k)$ in Figure 2 is indicative of the approximate equipartition of energy between kinetic and magnetic modes at small scales, the Alfvén effect described in section 2. The ratio $E_v(k)/E_B(k)$ lies in the range 0.4 to 1.2 as a function of k throughout the wave number interval. This is not atypical of the solar wind intervals we have examined. The total fluctuation magnetic and kinetic energies (per unit mass) are also nearly equal in this interval, with $E_B = 347 \text{ km}^2/\text{s}^2$ and $E_k = 325 \text{ km}^2/\text{s}^2$.

The overall degree of correlation between \mathbf{v} and \mathbf{B} is measured by the cross helicity, which is $H_c = 16 \text{ km}^2/\text{s}^2$ in this first interval. This is about 6% of $E/2$ which is the maximum absolute value possible for H_c . Based on this value of the total 'correlation coefficient' $2H_c/E \approx 0.06$, one might be tempted to conclude that this interval does not contain 'Alfvénic' fluctuations. A plot of twice the cross-helicity spectrum $2H_c(k)$, also in Figure 3, indicates that this

is not entirely true. The point is that H_c is not completely positive definite and although most of the modes have $H_c(k) > 0$, there are a number of modes for which $H_c(k) < 0$. In particular, there are two large negative values of $H_c(k)$ at very low wave number. As usual, the spectral estimates in the long-wavelength region have low statistical validity, but in this particular realization the few negative cross-helicity modes produce a substantial cancellation of the positive values. There are a number of wave number intervals for which $2H_c(k)/E(k) > 0.3$, indicating that some of the fluctuations are more 'Alfvénic' than the total correlation coefficient would suggest.

A spectrum of the magnetic helicity is given in Figures 4a and 4b. The magnetic helicity spectrum also takes on both positive and negative values, but there is no preferred sign at the small scales. The rapidly alternating sign of $H_m(k)$ produces cancellations throughout the spectrum, so that the net magnetic helicity is due only to the few lowest k (positive) contributions. The magnetic helicity spectrum can be compared with the energy spectrum using the ratio

$$\sigma(k) \equiv kH_m(k)/E_B(k) \quad (27)$$

which is bounded in absolute value by 1.

Figure 5 shows a plot of the first 700 of the 2500 points which comprise $\sigma(k)$. One interpretation of Figure 5 is that a substantial degree of helicity or circular polarization exists throughout the wave number spectrum, but the sense of polarization or handedness alternates randomly.

It should be noted that, in contrast to the energy spectrum, there is no well-established procedure for 'smoothing' or ensemble averaging nonpositive definite spectra such as $H_m(k)$ and $H_c(k)$. On the one hand, functions such as $\sigma(k)$ may be excessively smoothed to the point where $\sigma(k) \approx 0$ for almost all k , which would imply that the reduced spectra are either linearly polarized or unpolarized ($\sigma(k)$ does not measure linear polarization). These are properties not shared by any realization that comprises that ensemble. Even so, it is

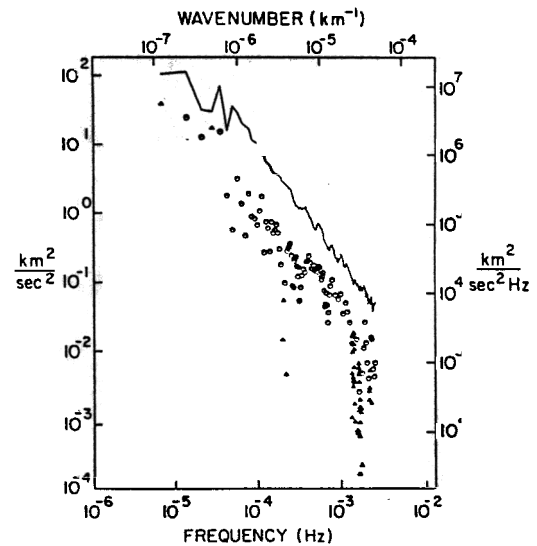


Fig. 3. Total energy spectrum (solid line) and twice the cross helicity spectrum (triangles are negative values; circles are positive values) for the 1 AU interval. The total cross helicity is positive, but two low-wave-number modes have negative cross helicity. The ordinate has units of $(\text{km/s})^2$.

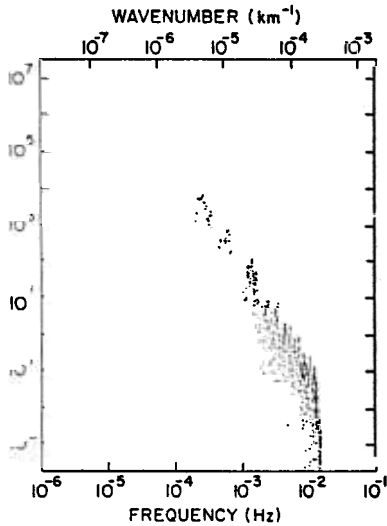


Fig. 4a. Scatter plot of the positive values of the magnetic helicity spectrum, in γ^2 km, for the 1 AU interval.

doubtful that any consistent averaging process would cause the large-scale magnetic helicity to vanish. At the other extreme, one might decide not to smooth H_m at all. The values of the unsmoothed $\sigma(k)$ (not shown here) are uniformly distributed between ± 1 throughout the entire spectrum. We have examined the Fourier transform of the unsmoothed $\sigma(k)$ and found that it has a nearly white noise spectrum, which suggests that the handedness of the fluctuations in a given wave number interval is substantial but uncorrelated with the handedness of fluctuations at nearby wave numbers. The unsmoothed $\sigma(k)$ has a low statistical weight, but we believe it accurately portrays the state of a particular realization, i.e., a particular data set.

In the present analysis, plots of $H_m(k)$ and $\sigma(k)$ have been 'smoothed' by the same procedures and to the same extent as has been used to bring the Blackman-Tukey and fast Fourier transform energy spectra (Figure 2) into agreement. The reader should note that Figure 5 contains overlaid plots from both the Blackman-Tukey (thicker line) and fast Fourier

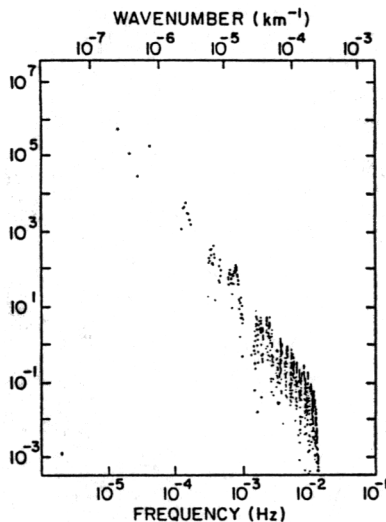


Fig. 4b. Scatter plot of the negative values of the magnetic helicity spectrum, in γ^2 km, for the 1 AU data.

er transform (thin line) analyses. The agreement indicates that our analysis techniques are stable and represent a valid description of the state of helical structures in the solar wind.

The magnetic helicity correlation length (18) for this interval is $\lambda_H = 1.7 \times 10^{11}$ cm, which is comparable to the correlation length of the magnetic fluctuations. Other lengths may be defined as generalizations of the one-dimensional Taylor microscale (26) by calculating moments of $H_m(k)$ in wave number space and normalizing by the total value of H_m . For example, consider λ_{1H} defined as

$$\lambda_{1H} \equiv 2\pi H_m / \left(\sum k H_m(k) \right) = 2.3 \times 10^{12} \text{ cm} \quad (28a)$$

$k > 0$

This may be compared with the similar quantity for the fluctuating magnetic energy, namely,

$$\lambda_{1E} \equiv 2\pi E_B / \left(\sum k E_B(k) \right) = 1.08 \times 10^{11} \text{ cm} \quad (28b)$$

$k > 0$

The k^2 moment of $H_m(k)$ (compare (26)) gives a length of $\lambda_{2H} = 1.2 \times 10^{12}$ cm, whereas the one-dimensional Taylor microscale for this interval is $\lambda = 3.2 \times 10^{10}$ cm. In each case we see that the lengths characterizing the helical part of the magnetic structures are of the order of or larger than those characterizing the magnetic structures themselves.

2.8 AU

The second interval was obtained by Voyager 2 at 2.8 AU on days 95–99 of 1978 (April 5–9). During this period the mean solar wind speed was 442 km/s and the spacecraft was in a high-speed stream just behind the stream interface. The analysis was done on 96-s plasma data samples and 48-s averages of the magnetometer data filtered and decimated so that the basic time interval was 144 s. We show only the results obtained using the fast Fourier transform technique.

The mean magnetic field in this interval lies in the ecliptic plane at an angle of about 66° away from \hat{R} and has a strength of 8.18 km/s (in Alfvén speed units). The mean plasma density was 0.545 proton/cm³ with an additional contribution

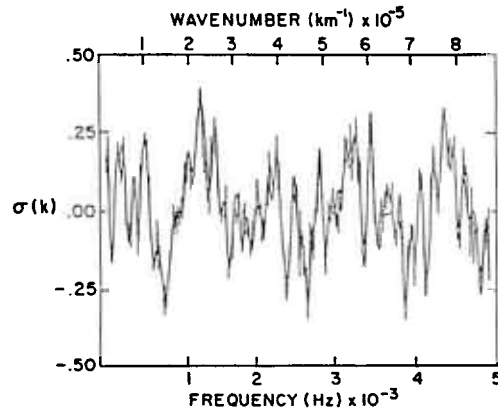


Fig. 5. Plot of $\sigma(k) \equiv k H_m(k) / E_B(k)$ versus frequency and wave number for the first 700 wave numbers of the spectra (in Figures 2, 4a, and 4b) from the 1 AU data. The values of $\sigma(k)$ from the Blackman-Tukey method are the thicker line; the fast Fourier transform values are the thin line.

of 4% alpha particles. The fluctuating magnetic energy density was $1.21 \gamma^2$ or $1.05 \times 10^3 \text{ km}^2/\text{s}^2$. This is greater than the value of fluctuating kinetic energy per unit mass, $E_v = 3.91 \times 10^2 \text{ km}^2/\text{s}^2$. This differential may be due in part to a decreasing trend in the proton density during the early part of the interval when the magnetic field also exhibited its largest fluctuations. Consequently, we may have overestimated b by a constant factor in converting to Alfvén speed units.

Figure 6 shows a plot of the total energy spectrum $E(k)$ as well as twice the cross-helicity spectrum $H_c(k)$. (In this plot we have further averaged the higher decades so that the individual symbols are clearly visible.) The energy spectrum again displays a nearly power law wave number dependence. A least squares fit to 800 points excluding the 50 lowest wave numbers gives a dependence of $k^{-1.67 \pm 0.17}$. The correlation length of the total energy is $1.0 \times 10^{12} \text{ cm}$. When calculated separately, the correlation length of the magnetic fluctuations is about 15% smaller than that of the velocity fluctuations. The one-dimensional Taylor microscale for the total energy is $6.8 \times 10^{10} \text{ cm}$.

The total cross helicity of the fluctuations is $H_c = -160 \text{ km}^2/\text{s}^2$ which gives a value of $[2H_c/E] \approx 0.11$. The spectrum of H_c (Figure 6) reveals that the cross helicity is one signed (negative) throughout most of the spectrum, but a few low k modes have substantial positive values. Again, we are led to the conclusion that the small-scale fluctuations are rather 'Alfvénic.' The extent of correlation between \mathbf{v} and \mathbf{B} in various portions of the spectrum may be seen by plotting

$$\sigma_{Hc}(k) = 2H_c(k)/E(k) \quad (29)$$

where $|\sigma_{Hc}| \leq 1$. Figure 7 shows $\sigma_{Hc}(k)$ for all but the lowest 10 wave numbers for this interval. It is clear that $\sigma_{Hc}(k) = -0.6$ to -0.8 for almost all wave numbers indicating a substantial anticorrelation of velocity and magnetic fields throughout most of the spectrum.

Several length scales can be calculated from the cross-helicity spectrum in analogy with the previously defined

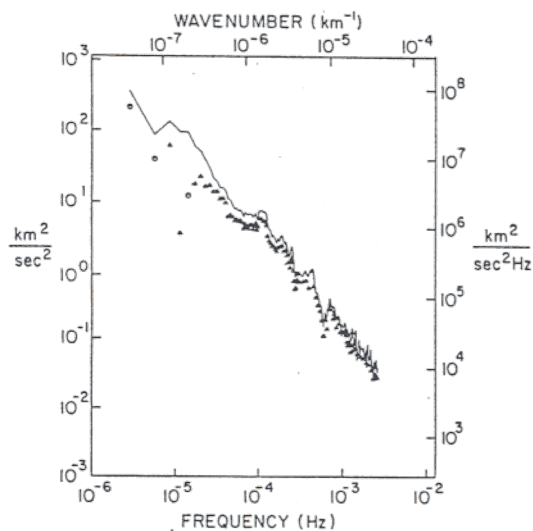


Fig. 6. Total energy spectrum (solid line) and twice the cross-helicity spectrum (circles are positive values and triangles are negative values) for the 2.8 AU data interval. Units are $(\text{km/s})^2$. In the high-wave-number region the fluctuations are nearly 'Alfvénic,' with negative velocity-magnetic field correlation. There are several large-scale positive cross-helicity modes.

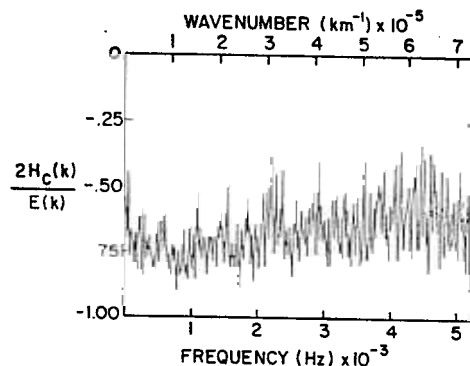


Fig. 7. Plot of $\sigma_{Hc}(k) = 2H_c(k)/E(k)$ versus k for the 2.8 AU data set. The lowest 10 wave numbers have been omitted to emphasize the degree of \mathbf{v} - \mathbf{B} correlation at high wave numbers.

correlation length, microscale and first moment (λ_{IE} , $(28b)$). These tend to be larger than the corresponding lengths calculated from the energy spectrum (see Table 1).

The cross-helicity spectra obtained from both of the first two intervals closely resemble similar measurements first reported by *Belcher and Davis* [1971] and *Coleman* [1966, 1967] in that the correlation is either positive definite or negative definite throughout most of the wave number range. When discussing the next interval, we shall see that this is not universally true.

In Figure 8 we plot the ratio

$$r_A(k) \equiv E_v(k)/E_B(k)$$

for this interval. This is a measure of the Alfvén effect discussed above (see section 2). Typical values of r_A lie near 0.4 to 0.8 for most of this spectrum. The extent to which this ratio is artificially reduced by variations in the density within the interval is uncertain, but the oscillation of $r_A(k)$ about a well-defined mean appears to be typical in the intervals so far examined. Alternatively, our neglect of pressure anisotropies in the fluid [see *Barnes*, 1979] may explain why r_A does not actually fluctuate about one.

The last rugged invariant we examine for this interval is the magnetic helicity. A convenient comparison of the magnetic helicity and energy spectra results if the magnetic helicity is multiplied by wave number so that it has the same dimensions as $E_B(k)$. Plots of $|kH_m(k)|$ and $E_B(k)$ are given in

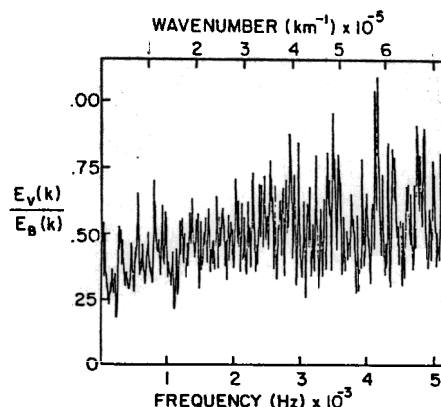


Fig. 8. The 'Alfvén effect ratio' $r_A = E_v(k)/E_B(k)$ versus k for the 2.8 AU data.

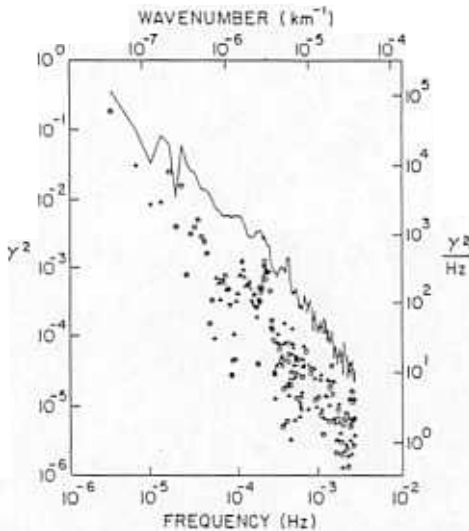


Fig. 9. Magnetic energy spectrum (solid line) and values of $|kH_m(k)|$ (circles are positive values; triangles are negative values) for the 2.8 AU data. The total H_m is positive.

Figure 9. Plotted in this way, the helicity curve is bounded from above by the energy. Positive and negative values of $kH_m(k)$ are plotted with different symbols so that information is not lost by taking the absolute value. Extensive averaging has been done in the last 2 decades in k to enable one to distinguish the two symbols. Note that the envelope of $|kH_m(k)|$ appears to follow the same power law as $E(k)$, indicating that for this interval as well as in the 1 AU data set $|kH_m(k)|$ does not go to zero in a regular way for large k . In Figure 10 we have plotted $\sigma(k)$ for this interval. It can be seen that $|\sigma(k)|$ exceeds 0.4 in several places, which indicates a two-to-one dominance of right circular polarization over left (or vice versa) in the context of a slab model. Again the total magnetic helicity ($H_m = 3.9 \times 10^{11} \gamma^2 \text{ cm}$) is due entirely to contributions from small k because the oscillations at large k tend to cancel.

The various characteristic lengths of the helicity indicate that this spectrum is also dominated by long-wavelength contributions, as was the case at 1 AU. In this case, $\lambda_H = 2.0 \times 10^{12} \text{ cm}$ is somewhat greater than the magnetic correlation length ($1.06 \times 10^{12} \text{ cm}$). Surprisingly, $\lambda_{2H} = 4.6 \times 10^{12} \text{ cm}$ exceeds the correlation length and is much greater than its

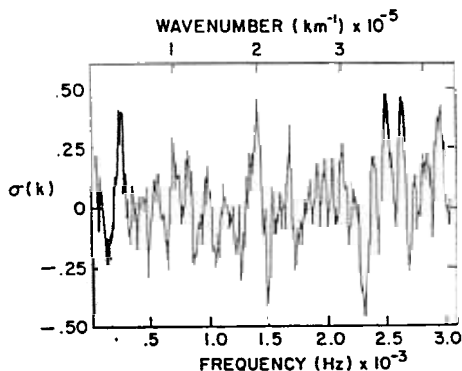


Fig. 10. The normalized measure of magnetic helicity, $\sigma(k) = kH_m(k)/E_H(k)$ versus k for the 2.8 AU data set. The 10 lowest wave number values have been omitted. A total of 950 wave numbers are included. Substantial polarizations occur throughout the spectrum.

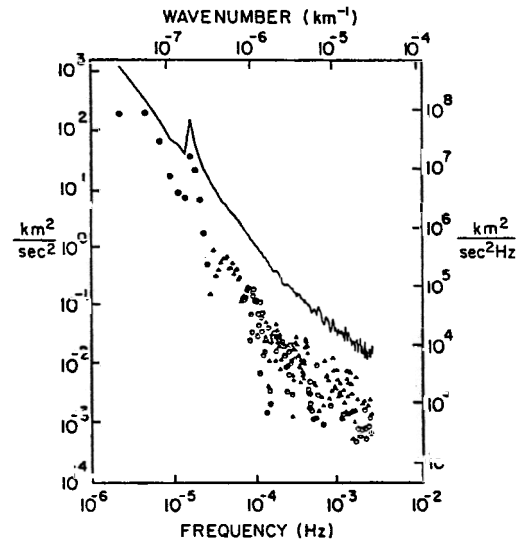


Fig. 11. Total energy spectrum (solid line) and twice the cross-helicity spectrum (circles are positive values and triangles are negative values) in units of $(\text{km/s})^2$ for the 5 AU data set. The total cross helicity is positive and is due primarily to the low-wave-number contributions. The high-wave-number cross helicities are of mixed sign, in contrast to the results at 1 and 2.8 AU shown in Figures 4 and 7.

analogue, the one-dimensional magnetic Taylor microscale $\lambda = 1.3 \times 10^{11} \text{ cm}$. Note that if all the helicity was found at only one wave number, then one might expect that λ_H , λ_{1H} , and λ_{2H} would all be equal. The fact that they lie within a factor of 5 suggests that for this interval the helicity spectrum is completely dominated by contributions from wavelengths greater than 10^{12} cm and that the contributions at all other scales have averaged out.

5 AU

Finally, we briefly present an analysis of a Voyager 1 data taken from January 6–10, 1979, 3 months before Jupiter encounter. During this interval Voyager 1 was in a stream rarefaction region. The solar wind speed decreased during this 5-day interval from 580 km/s to 430 km/s.

Figure 11 shows both the total energy spectrum $E(k)$ and twice the cross-helicity spectrum $H_c(k)$. The energy spec-

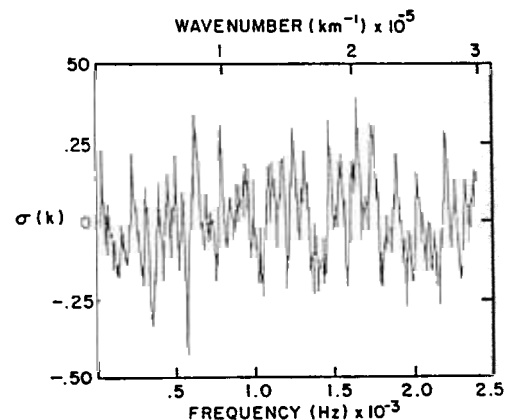


Fig. 12. The normalized magnetic helicity, $\sigma(k) = kH_m(k)/E_H(k)$ for the 5 AU data. The lowest 10 wave numbers are omitted and the next 1000 lowest are plotted. Both positive and negative magnetic helicity are found throughout the spectrum.

trum is again a power law with a slope of -1.70 ± 0.03 over the range from several times 10^{-5} Hz to about 10^{-3} Hz. The spectrum then tends to become flatter at higher frequencies, perhaps due to aliasing close to the Nyquist frequency of 5×10^{-3} Hz. The cross-helicity spectrum in the figure is particularly notable because it is dissimilar to those shown previously (Figures 3 and 6), where we had seen a nearly pure sign of $H_c(k)$ at all but the lowest wave numbers. But in this spectrum the first 10 or so wave numbers have the same sign, and subsequently, $H_c(k)$ oscillates about 0. This is in contrast to the type of correlation previously reported by *Belcher and Davis* [1971] and to the other intervals described above. The degree of correlation is greater for the larger scales than for the high k fluctuations where the correlation is not very great.

The magnetic helicity spectrum for this interval is quite similar to those described before. Figure 12 shows 1000 points of $\sigma(k)$ from the magnetic field analysis of this interval. Once again, the sense of handedness alternates as a function of k . The major contribution to the total magnetic helicity is, as before, due to the large-scale fluctuations.

6. DISCUSSION AND CONCLUSIONS

In the preceding sections we have described an analysis technique for obtaining the energy, cross helicity, and magnetic helicity spectra of MHD scale solar wind fluctuations. The method used is appropriate for homogeneous fluctuations and makes use of the 'frozen-in' property which is well satisfied for the super-Alfvénic flow typical of the solar wind. In a nonideal flow such as the solar wind the three invariants impose important constraints on nonlinear dynamics. Their wave number spectra are a natural way, from the point of view of turbulence theory, to describe the state of the system.

In section 5, results of application of our technique to Voyager data have been presented. The number of intervals analyzed is not so large that an exhaustive sampling of solar wind conditions could be claimed. Nonetheless, the results presented appear to us to be typical.

The energy spectra we find closely resemble the power law spectra reported by many others. The power law indices found in the three intervals discussed above are consistent with a $k^{-5/3}$ dependence and inconsistent, to within the quoted statistical error, with either k^{-2} or $k^{-3/2}$. This result for an MHD fluid is strikingly reminiscent of the results found for fluid turbulence in a tidal channel reported by *Grant et al.* [1962]. We hesitate to conclude whether the solar wind more closely resembles the predictions of Kolmogoroff for hydrodynamic turbulence (i.e., a $-5/3$ spectral index) or the predictions of Kraichnan for MHD media (i.e., a $-3/2$ spectral index). For one thing classical turbulence analysis has succeeded in predicting power law dependence of the omnidirectional spectrum only by assuming isotropic symmetry and spatial homogeneity. The solar wind may be more or less homogeneous, but the magnetic fluctuations certainly do not have isotropic symmetry [*Belcher and Davis*, 1971]. Magnetic fluctuations tend to have minimum variance in nearly the same direction as the mean magnetic field (see, for example, the review by *Barnes* [1979]). This indicates anisotropy and also suggests that the mean magnetic field introduces a preferred direction into the energy spectrum tensor. This invalidates the assumptions of the usual *Kolmogoroff* [1941] or *Kraichnan* [1965] dimensional

arguments. We know of no theoretical derivation that gives a spectral prediction for anisotropic geometry. Furthermore, even if such a prediction existed, one-dimensional reduced spectra do not permit unraveling the k dependence in an unambiguous fashion [*Fredricks and Coroniti*, 1976]. Power law indices of interplanetary magnetic fluctuations are not always nearly $-5/3$; for example, *Sari and Valley* [1976] have reported values ranging from -1 to -2 .

The correlation lengths obtained fall in the range 1 to 30×10^{11} cm. It is difficult to attach great validity to these values because of the sensitivity of the measurement to very low wave number power (Appendix B) where the spectral estimates are not generally known with high statistical certainty. However, the values we find tend to be larger than the canonical value of 2×10^{11} cm (or even 2×10^{10} cm [*Fisk and Sari*, 1973]) used in the study of cosmic ray propagation in the heliosphere [*Jokipii*, 1966; *Jokipii and Coleman*, 1968; *Sari and Ness*, 1969] and often equal or exceed the 10^{12} cm found by *Hedgecock* [1975]. This difference may be a result of the rather long data intervals that both *Hedgecock* and we have used.

The cross-helicity (and Alfvén effect ratio) measurements are sensitive to the assumption of incompressibility. All the measurements in this paper have used the mean density of the interval to normalize the magnetic field to Alfvén speed units. We have found that in most intervals normalization by the instantaneous density gives larger cross helicities and moves the ratio $r_A = E_v(k)/E_B(k)$ toward unity. It is also possible [*Barnes*, 1979] to define quantities similar to cross helicity which are diagnostic of small-amplitude Alfvén waves in the presence of pressure anisotropies and variable density. We have chosen not to incorporate such complications into our analysis as they lead away from the simple MHD turbulence model that forms the basis of our approach. There is no theory of fully developed MHD turbulence that includes either compressive effects or pressure anisotropies.

The cross-helicity spectra of the 1 AU and 2.8 AU intervals (Figures 3, 6, and 7) indicate the presence of 'Alfvénic' fluctuations, because of the single sign of H_c over much of the spectrum. The sign of this correlation corresponds to 'outward propagating Alfvénic fluctuations.' The small number of modes with the opposite sign of $H_c(k)$ (some of which have a substantial amplitude) represent 'inward travelling' Alfvénic fluctuations. These have not been reported previously [*Barnes*, 1979] and may complicate the usual interpretation that the outward propagating fluctuations represent the residue of coronal waves being convected outward (see, for example, the review by *Hollweg* [1978]).

There is a possibility that the type of 'Alfvénic' spectra seen in the 1 and 2.8 AU data sets may be explained in a way that does not appeal to the notion of propagating structures. For example, *Dobrowolny et al.* [1980b], using the approach of *Kraichnan* [1965], have suggested that MHD turbulence tends to amplify correlations between velocity and magnetic fields. To some extent this has been verified in two-dimensional computer simulations (W. H. Matthaeus and D. Montgomery, unpublished data, 1981) and closure calculations [*Frisch et al.*, 1981; *Grappin et al.*, 1982]. In the wave interpretation the source of cross helicity is assumed to be near the sun where only outward propagating waves are able to pass the transonic point in the corona. An alternative source of H_c may be the cross helicity of the mean field, that

is, $V_{\text{sw}} \cdot \mathbf{B}_0$, which is in general nonzero. Especially if the large-scale shear in V_{sw} is an energy source for driving turbulence, it may also be a source of cross helicity. It appears that neither the wave nor turbulence interpretations have been developed sufficiently to explain the details of the observed cross-helicity spectra of 'Alfvénic periods.'

The cross-helicity spectrum derived from the third interval taken at 5 AU is not 'Alfvénic' in the usual sense. The small k modes exhibit a cross-helicity corresponding in sign to outward travelling waves, but the sign of $H_c(k)$ is mixed for the remainder of the spectrum. To our knowledge, this type of mixed spectrum has not been seen before [Barnes, 1979]. As we pointed out in section 5, this period is characterized by a large decrease in the solar wind speed. The uniqueness of this cross-helicity spectrum may be a consequence of its being acquired in a strong rarefaction region. It should be noted that there has not yet been any systematic study of the properties of Alfvénic fluctuations at large heliocentric distance and our observations may reflect the evolution of Alfvénic turbulence over time and distance. Because this is the only rarefaction region that we have analyzed thus far, we cannot reach any general conclusions.

In contrast to the variety of cross-helicity spectra we have seen in our limited sample, every interval of solar wind data we have analyzed has displayed a magnetic helicity spectrum of the type shown in our spectral plots. The only exceptions have been the days prior to Jupiter encounter on Voyager 1 when upstream waves were noticeably present. A detailed analysis of that period has been presented by Smith *et al.* [1982]. The typical spectrum of $H_m(k)$ as seen in the solar wind far from planetary bow shock interference has an alternating sign throughout the sampled wave number spectrum but is dominated in magnitude by contributions from scales of the order of or greater than the magnetic correlation length. This is reminiscent of the predictions of the inverse cascade and selective decay hypotheses, which predict that magnetic helicity is preferentially transferred to large spatial scales by turbulent MHD behavior. Parker [1972] has also argued that equilibrium magnetic fields should display a large-scale uniform twist. These predictions are consistent with our finding that the characteristic helicity lengths are greater than the corresponding lengths characterizing the distribution of energy.

The small-scale appearance of the magnetic helicity spectrum is more difficult to interpret. The spectra we have obtained have large values of $\sigma(k)$ (27) throughout the spectrum. Thus the fluctuations appear to have a random, uncorrelated sense of circular polarization at all small scales. Previously, Goldstein and Matthaeus [1981] have argued that including unsmoothed $H_m(k)$ in calculation of the mean free path of charged particles can substantially increase the mean free path, at least in slab geometry. However, it is clear that this result needs to be carefully investigated, if only because the quasi-linear theory of charged particle transport presupposes an ensemble average of the statistical quantities in the derivation of the spatial transport coefficient (for example, see the review by Völk [1975]). An alternative point of view (J. R. Jokipii, private communication, 1981) is that ensemble averaging reduces the high k values of $\sigma(k)$ to near zero, so that charged particle propagation would be unaffected by the small-scale magnetic helicity. This issue remains undecided.

Interpretation of the dominant contribution to the magnet-

ic helicity, due to fluctuations whose scale is of the order of, or greater than, the correlation length, is more straightforward. Let us imagine that the solar wind magnetic field is composed of a large number of flux tubes all of which are aligned with the Parker spiral pattern. Our measurements suggest that within each flux tube the longest wavelength fluctuations are nonmirror symmetric. In turbulence theory, long-wavelength fluctuations are estimated to evolve slowly as can be seen from the 'eddy turnover time' (see section 4) or from an analogy to the hydrodynamic phenomenon known as the 'permanence of big eddies' [Batchelor, 1970]. Thus such large-scale helical components of the field will evolve so slowly that for many purposes they can be thought of as comprising part of the mean field itself. In this way the 'mean' field within each of our imaginary flux tubes is a helix with its axis along the Parker spiral, while neighboring flux tubes have similar structure but perhaps with different net helicity. Candidates for the lateral flux tube extent include the distances between sector boundaries or, perhaps, the separation between tangential discontinuities (see, for example, the recent work of Lee and Fisk [1981]). However, the scale size that we find characterizes the helicity is systematically larger ($\approx 10^{12}$ cm) than the typical separation of tangential discontinuities ($\approx 10^{11}$ cm) [Fisk and Sari, 1973], suggesting that the origin of the large-scale helical structure of the solar wind field lies elsewhere.

The purpose of this paper has been to illustrate a technique for measuring the three rugged invariants of MHD in the solar wind. Further analysis of more intervals is necessary to derive a more statistically relevant picture of 'typical' solar wind conditions. Data are now available out to ≈ 11 AU, which should permit further study of turbulent processes and comparison with selective decay and inverse cascade hypotheses in a more quantitative way than has been attempted here.

APPENDIX A: UNITS

The equations of MHD ((1)–(4) in section 2) have been written in a simplified form by introducing the magnetic field \mathbf{b} in Alfvén speed units, where $\mathbf{b} = \mathbf{B}/[(4\pi\rho_0)^{1/2}]$. \mathbf{B} is the usual magnetic field and ρ_0 is the mean density. Written in this way, the MHD equations can be immediately related to a system of dimensionless units [Fyfe and Montgomery, 1976] which is summarized here.

An arbitrary length scale L_0 and an arbitrary magnetic field scale B_0 are introduced. Ordinarily, L_0 may be chosen to be a boundary separation or a measure of the size of a typical energy containing magnetic structure, such as the correlation length. The magnetic unit B_0 is in Alfvén speed units; thus a time scale $T_0 = L_0/B_0$ is automatically defined and is the 'Alfvén transit time of unit distance' often quoted in numerical simulation work.

The natural units of electric current density become B_0/L_0 and the units of velocity are, of course, $V_0 = B_0$, the unit Alfvén speed. It is easy to see that all of the terms in (1) and (2) become dimensionless in these units.

The dimensional viscosity per unit mass ν is replaced by the dimensionless reciprocal Reynolds number $1/R = \nu/B_0L_0$. Similarly, the dimensional resistivity μ is replaced by $1/R_L = \mu/B_0L_0$, the magnetic Lundquist number [Shercliff, 1965]. When kinetic and magnetic energies are nearly equal, then B_0 is the characteristic velocity of the system and R_L becomes the magnetic Reynolds number μ/V_0L_0 .

APPENDIX B: SPECTRA AND CORRELATION FUNCTIONS IN HOMOGENEOUS FLUCTUATIONS

If a correlation function $R'(r)$ vanishes sufficiently rapidly at large r , it may be well approximated by a function $R(r)$ satisfying

$$R(r) = R'(r) \quad r < L_0$$

and

$$R(r) = 0 \quad r > L_0$$

for some L_0 . We refer to such functions as 'Lanczos-type' [Lanczos, 1956]. For such functions there is an exact correspondence between their Fourier series and Fourier transforms, which is

$$\tilde{S}(k) = k_{\min} S(k) \quad (\text{B1})$$

where \tilde{S} is the Fourier series representation of $R(r)$ evaluated with an assumed periodicity length of $2L$ and $k_{\min} = \pi/L$ is the minimum wave number in the Fourier series. In writing (B1) it is assumed that $L > L_0$ and that $S(k)$ is evaluated only at the same discrete wave numbers present in the Fourier series, $\tilde{S}(k)$. The correlation length is

$$L_c = \int_0^L R(r) dr \quad (\text{B2})$$

The upper limit has been reduced from infinity to L without error, and we have normalized R by the 'energy' so that $R(0) = 1$. Because $|R(r)| \leq R(0)$, it follows that $L_0 \geq L_c$.

Consider the spectrum of R calculated from

$$\tilde{S}(k) = (1/2L) \int_{-L}^{+L} R(r) \exp -ikr$$

If $\tilde{S}(k)$ is evaluated at any wave number such that $k' < 2\pi/L_0$, then

$$\tilde{S}(k' < 2\pi/L_0) = (k_{\min}/\pi)[L_c + O((k'L_0)^2)] \quad (\text{B3})$$

Thus the low-wave-number spectrum of a Lanczos-type function goes to a constant proportional to the correlation length.

A model correlation function with the correct asymptotic behavior as $k \rightarrow 0$ is

$$R(r) = \exp - (r/L_c)$$

This form may be used to estimate the error introduced by assuming that $R(r > L_0) = 0$. This form has often been used as an approximate means of estimating L_c in lieu of evaluating (B2) (see, for example, Sari and Valley [1976]) and will be essentially exact for $1/k^2$ power spectra.

Suppose that the Lanczos cutoff length L_0 is greater than L_c and that the true correlation function $R(r) = \exp - (r/L_c)$ for $r > L_0$, then S^* the exact Fourier transform of the correlation function is related to S , calculated under the assumption that R is Lanczos type by

$$S(k) = S^*(k) - (1/\pi) \frac{L_c}{1 + k^2 L_c^2} \exp - (L_0/L_c + ikL_0)$$

Notice that for high k fluctuations ($k \gg 2\pi/L_c$), the error introduced by taking $L_0 = L_c$ is $O(1/(kL_c)^2)$. On the other hand, when $L_0 > L_c$, the error exponentially decreases as $\exp - (L_0/L_c)$. Thus so long as $R \ll 1$ at the maximum

calculated lag (assuming that the total interval includes at least several correlation lengths), meaningful spectra can be obtained from solar wind data. It makes little difference whether the correlation functions are obtained from a strictly periodic system, a strictly homogeneous system, or a real inhomogeneous system which has correlation functions of the Lanczos type. Of course, homogeneity in the 'weak' mathematical sense requires the more stringent condition that the mean fields and correlation functions be translation invariant (9). However, these properties pertain only to the entire ensemble under consideration. Any finite length sample of a homogeneous ensemble is expected to contain low-wave-number fluctuations satisfying (B3). 'Trends' in the mean field and variance of a data set can to some extent be included in the analysis without introducing inconsistency with the notion of a homogeneous ensemble.

These conclusions apply equally well to evaluation of the off-diagonal elements of the correlation matrix (and therefore the magnetic helicity spectrum) if L_c is replaced by L_H (section 3) and $R(r)$ is replaced by $\phi(r)$, the helicity 'generating function.'

Acknowledgments. The authors would like to thank the members of the Voyager magnetometer and plasma teams for their support during this project. In particular, the advice of M. Acuña, L. Burlaga, J. D. Scudder, and J. Belcher was especially helpful. The aid of W. H. Mish and others in the Information Analysis and Display Branch with the spectral analysis programs was invaluable. C. W. Smith is acknowledged for his help with the cross-helicity programs. This research was supported, in part, by NASA's Solar and Terrestrial Theory Program and motivated, in part, by the Report of the NASA Plasma Turbulence Explorer Study Group. During the course of this research, W.H.M. was a NAS/NRC resident postdoctoral research associate.

The Editor thanks A. Barnes, M. Dobrowolny, and D. Montgomery for their assistance in evaluating this paper.

REFERENCES

- Barnes, A., Hydromagnetic waves and turbulence in the solar wind, in *Solar System Plasma Physics*, edited by C. F. Kennel, L. J. Lanzerotti, and E. N. Parker, vol. 1, North-Holland, Amsterdam, 1979.
- Batchelor, G. K., *Theory of Homogeneous Turbulence*, Cambridge University Press, New York, 1970.
- Behannon, K., Heliocentric distance dependence of the interplanetary magnetic field, *Rev. Geophys. Space Phys.*, 16, 125, 1978.
- Behannon, K., M. H. Acuña, L. F. Burlaga, R. P. Lepping, N. F. Ness, and F. M. Neubauer, Magnetic field experiment for Voyagers 1 and 2, *Space Sci. Rev.*, 21, 235, 1977.
- Belcher, J. W., and L. Davis, Large-amplitude Alfvén waves in the interplanetary medium, 2, *J. Geophys. Res.*, 76, 3534, 1971.
- Blackman, R., and J. Tukey, *Measurement of Power Spectra*, Dover, New York, 1958.
- Bridge, H. S., J. W. Belcher, R. J. Butler, A. J. Lazarus, A. M. Mauretic, J. D. Sullivan, G. L. Siscoe, and V. M. Vasyliunas, The plasma experiment on the 1977 Voyager mission, *Space Sci. Rev.*, 21, 259, 1977.
- Burlaga, L. F., and J. M. Turner, Microscale 'Alfvén waves' in the solar wind at 1 AU, *J. Geophys. Res.*, 81, 73, 1976.
- Chandrasekhar, S., The theory of axisymmetric turbulence, *Philos. Trans. R. Soc. London Ser. A*, 242, 557, 1951.
- Chang, S. C., and A. Nishida, Spatial structure of transverse oscillations in the interplanetary magnetic field, *Astrophys. Space Sci.*, 23, 301, 1973.
- Chu, C., Magnetic spectra and electron transport of current carrying plasmas, *Phys. Rev. Lett.*, 48, 246, 1982.
- Coleman, P. J., Hydromagnetic waves in the interplanetary medium, *Phys. Rev. Lett.*, 17, 207, 1966.
- Coleman, P. J., Wave-like phenomena in the interplanetary medium, *Planet. Space Sci.*, 15, 953, 1967.

- Coleman, P. J., Turbulence, viscosity and dissipation in the solar wind plasma, *Astrophys. J.*, **153**, 371, 1968.
- Cowling, T. G., *Magnetohydrodynamics*, Adam Hilger, Ltd., Bristol, England, 1976.
- Cramér, H., On the theory of stationary random processes, *Ann. Math.*, **41**, 215, 1940.
- Dobrowolny, M., A. Mangeney, and P. Veltri, Properties of magnetohydrodynamic turbulence in the solar wind, *Astron. Astrophys.*, **83**, 26, 1980a.
- Dobrowolny, M., A. Mangeney, and P. Veltri, Fully developed anisotropic hydromagnetic turbulence in interplanetary space, *Phys. Rev. Lett.*, **45**, 144, 1980b.
- Elsasser, W. M., Hydromagnetic dynamo theory, *Rev. Mod. Phys.*, **18**, 135, 1956.
- Fisk, L., and J. Sari, Correlation length for interplanetary magnetic field fluctuations, *J. Geophys. Res.*, **78**, 6729, 1973.
- Fredricks, R. W., and F. V. Coroniti, Ambiguities in the deduction of rest frame fluctuation spectrums from spectrums computed in moving frames, *J. Geophys. Res.*, **81**, 5591, 1976.
- Frisch, U., A. Pouquet, J. Léorat, and A. Mazure, Possibility of an inverse cascade of magnetic helicity in magnetohydrodynamic turbulence, *J. Fluid Mech.*, **68**, 769, 1975.
- Frisch, U., M. Meneguzzi, and A. Pouquet, Turbulence et champs magnétiques, in *Image de la Physique*, p. 27, Centre National de la Recherche Scientifique, Paris, 1981.
- Fyfe, D., and D. Montgomery, High beta turbulence in two dimensional magnetohydrodynamics, *J. Plasma Phys.*, **16**, 181, 1976.
- Fyfe, D., D. Montgomery, and G. Joyce, Dissipative forced turbulence in two dimensional magnetohydrodynamics, *J. Plasma Phys.*, **17**, 369, 1977.
- Goldstein, M. L., and W. H. Matthaeus, The role of magnetic helicity in cosmic ray transport theory, *Proc. Int. Conf. Cosmic Rays 17th*, **3**, 204, 1981.
- Goldstein, M. L., A. J. Klimas, and F. D. Barish, On the theory of large amplitude Alfvén waves, in *Solar Wind Three*, edited by C. T. Russell, university of California Press, Los Angeles, 1974.
- Grant, H. L., R. W. Stewart, and A. Moilliet, Turbulence spectra from a tidal channel, *J. Fluid Mech.*, **12**, 241, 1962.
- Grappin, R., U. Frisch, L. Léorat, and A. Pouquet, Alfvénic fluctuations as asymptotic states of MHD turbulence, *Astron. Astrophys.*, **105**, 6, 1982.
- Hamming, R. W., *Numerical Methods for Scientists and Engineers*, McGraw-Hill, New York, 1973.
- Hedgecock, P. C., Measurements of the interplanetary magnetic field in relation to the modulation of cosmic rays, *Sol. Phys.*, **42**, 497, 1975.
- Hollweg, J. V., Some physical processes in the solar wind, *Rev. Geophys. Space Phys.*, **16**, 689, 1978.
- Holzer, T. E., The solar wind and related astrophysical phenomena, in *Solar System Plasma Physics*, edited by C. F. Kennel, L. J. Lanzerotti, and E. N. Parker, vol. 1, North-Holland, Amsterdam, 1979.
- Hundhausen, A. J., *Coronal Expansion and Solar Wind*, Springer-Verlag, New York, 1972.
- Jokipii, J. R., Cosmic ray propagation, 1, Charged particles in a random magnetic field, *Astrophys. J.*, **146**, 480, 1966.
- Jokipii, J. R., and P. J. Coleman, Cosmic ray diffusion tensor and its variation observed with Mariner, 4, *J. Geophys. Res.*, **73**, 5495, 1968.
- Kolmogoroff, A. N., The local structure of turbulence in incompressible viscous fluid for very large Reynolds numbers, *C. R. Acad. Sci. URSS*, **30**, 201, 1941.
- Kraichnan, R. H., Inertial range of hydromagnetic turbulence, *Phys. Fluids*, **8**, 1385, 1965.
- Kraichnan, R. H., Inertial ranges in two dimensional turbulence, *Phys. Fluids*, **10**, 1417, 1967.
- Kraichnan, R. H., and D. C. Montgomery, Two dimensional turbulence, *Rep. Prog. Phys.*, **43**, 547, 1980.
- Lanczos, C., *Applied Analysis*, Prentice-Hall, Englewood Cliffs, N. J., 1956.
- Lee, M. A., and L. A. Fisk, The role of particle drifts in solar modulation, *Astrophys. J.*, **248**, 836, 1981.
- Matthaeus, W. H., and M. L. Goldstein, Stationarity of magnetohydrodynamic fluctuations in the solar wind, *NASA Tech. Memo.*, 83963, 1982.
- Matthaeus, W. H., and D. C. Montgomery, Selective decay hypothesis at high mechanical and magnetic Reynolds numbers, *Ann. N. Y. Acad. Sci.*, **357**, 203, 1980.
- Matthaeus, W. H., and D. Montgomery, Nonlinear evolution of the sheet pinch, *J. Plasma Phys.*, **25**, 11, 1981.
- Matthaeus, W. H., and C. Smith, The structure of correlation tensors in homogeneous anisotropic turbulence, *Phys. Rev. A*, **24**, 2135, 1981.
- Matthaeus, W. H., M. L. Goldstein, and C. Smith, Evaluation of magnetic helicity in homogeneous turbulence, *Phys. Rev. Lett.*, **48**, 1256, 1982.
- McClellan, J. H., T. W. Parks, and L. R. Rabiner, FIR linear phase filter design program, in *Programs for Digital Signal Processing*, IEEE Press, New York, 1979.
- Moffatt, H. K., *Magnetic Field Generation in Electrically Conducting Fluids*, Cambridge University Press, New York, 1978.
- Montgomery, D. C., and L. Turner, Anisotropic magnetohydrodynamic turbulence in a strong external magnetic field, *Phys. Fluids*, **24**, 825, 1981.
- Montgomery, D., L. Turner, and G. Vahala, Three dimensional magnetohydrodynamic turbulence in cylindrical geometry, *Phys. Fluids*, **21**, 757, 1978.
- Morf, R., S. A. Orszag, and U. Frisch, Spontaneous singularity in three dimensional, inviscid, incompressible flow, *Phys. Rev. Lett.*, **44**, 572, 1980.
- Orszag, S. A., Lectures on the statistical theory of turbulence, in *Fluid Dynamics, 1973 Les Houches Summer School of Theoretical Physics*, edited by R. Balian and J.-L. Peube, p. 235, Gordon and Breach, New York, 1977.
- Otnes, R. K., and L. Enochson, *Digital Time Series Analysis*, John Wiley, New York, 1972.
- Panchev, S., *Random Functions and Turbulence*, Pergamon, New York, 1971.
- Panofsky, W., and M. Phillips, *Classical Electricity and Magnetism*, Addison-Wesley, Reading, Mass., 1962.
- Parker, E. N., Topological dissipation and the small scale fields in turbulent gases, *Astrophys. J.*, **174**, 499, 1972.
- Parker, E. N., *Cosmical Magnetic Fields*, Clarendon, Oxford, 1979.
- Robertson, H. P., The invariant theory of isotropic turbulence, *Proc. Cambridge Philos. Soc.*, **36**, 209, 1940.
- Sari, J. W., and N. F. Ness, Power spectra of the interplanetary magnetic field, *Sol. Phys.*, **8**, 155, 1969.
- Sari, J. W., and G. C. Valley, Interplanetary magnetic field power spectra: Mean field radial or perpendicular to radial, *J. Geophys. Res.*, **81**, 5489, 1976.
- Shercliff, J. A., *A Textbook of Magnetohydrodynamics*, Pergamon, New York, 1965.
- Smith, C., M. L. Goldstein, and W. H. Matthaeus, Turbulence analysis of the Jovian upstream wave phenomenon, submitted to *J. Geophys. Res.*, 1982.
- Taylor, G. I., Statistical theory of turbulence, *Proc. R. Soc. London Ser. A*, **151**, 421, 1935.
- Taylor, G. I., The spectrum of turbulence, *Proc. R. Soc. London Ser. A*, **164**, 476, 1938.
- Taylor, J. B., Relaxation of toroidal plasma and generation of reverse magnetic fields, *Phys. Rev. Lett.*, **33**, 1139, 1974.
- Turner, L., and J. P. Christiansen, Incomplete relaxation of pinch discharges, *Phys. Fluids*, **24**, 893, 1981.
- Völk, H. J., Cosmic ray propagation in interplanetary space, *Rev. Geophys. Space Phys.*, **13**, 547, 1975.
- Walén, C., On the theory of subspots, *Ark. Mat. Astron. Fys.*, **30A(15)**, 31B(3), 1944.
- Woltjer, L., On hydromagnetic equilibrium, *Proc. Natl. Acad. Sci. USA*, **44**, 833, 1958a.
- Woltjer, L., A theorem on force free fields, *Proc. Natl. Acad. Sci. USA*, **44**, 489, 1958b.

(Received March 17, 1982;
revised May 10, 1982;
accepted May 10, 1982.)